Bacterial pathogens dynamic during multi-species infections

Marie-Anne Barny*, Sylvia Thieffry, Christelle Gomes de Faria, Elisa Thebault and Jacques Pédron

Sorbonne Université, INRAE, IRD, CNRS, UPEC, Institute of Ecology and Environmental Sciences-Paris (iEES-Paris), 4 place Jussieu, F-75252 Paris, France

**E-mail : marie-anne.barny@sorbonne-universite.fr*

Abstract

Soft rot *Pectobacteriacea* (SRP) gathers more than 30 bacterial species that collectively rot a wide range of plants by producing and secreting a large set of plant cell wall degrading enzymes (PCWDEs). Worldwide potato field surveys identified 15 different SRP species on symptomatic plants and tubers. The abundance of each species observed during outbreaks varies over space and time and the mechanisms driving species shift during outbreak are unknown. Furthermore, multi-species infections are frequently observed and the dynamics of these coinfections are not well understood.

To understand the dynamics of coinfections, we set up 16 different synthetic communities of 6 SRP strains to mimic coinfections. The bacteria present in each tested community were representative of 2 different species, with 3 strains per species. These communities were inoculated in potato tubers or on synthetic media and their outcome was followed by amplification and Illumina sequencing of the discriminatory housekeeping gene *gap*A. We also compared disease incidence and bacterial multiplication in potato tubers during mixed-species infection and single-species infection. A species that was unable to induce disease in potato was efficiently maintained and eventually became dominant in some of the communities tested, indicating that cheating can shape dominant species. Modeling indicates that the cost of PCWDEs production and secretion, the rate of potato degradation and the diffusion rate of degraded substrate could favor the cheater species. Interaction outcomes differed between potato tuber and synthetic medium, highlighting the driving effect of environmental conditions, with higher antagonistic interactions observed in potato tubers. Antagonistic interactions were strain specific and not species specific. Toxicity interference was also observed within some communities, allowing the maintenance of strains otherwise sensitive to toxic compounds. Overall, the results indicate that intraspecific competition, cooperation through trophic interaction and toxicity interference contribute to the maintenance of SRP diversity. The implications of these processes for epidemiological surveillance are discussed.

Introduction

Pathogenic bacteria developed specialized weapons to attack their host, subvert host defenses and gain nutrient to develop inside their host. Among pathogens, some are specialists with a narrow host range and infect a single host while others have the capacity to infect many different hosts. A mirrored situation occurred with disease, while many diseases are defined by a single well known pathogenic species, other diseases could be triggered by a complex of bacterial species that share common bacterial weapons and could act either individually and/or collectively during disease development. When a disease is triggered by a species complex many questions concerning the dynamic of the complex are still unsolved. Notably, it is unclear to what extend the different species involved compete, cheat, and cooperate within the symptoms. As well it is also unclear if cheating, competition and cooperation behavior mainly occurs at the strain level or at the species level. Furthermore, as each disease cycle involved many different steps, it is unclear to which extend the competition/cooperation game change with changing environmental conditions and to what extend these interactions are shaping the bacterial diversity of pathogens.

Plant pathogens with a broad host range, such as the soft rot *Pectobacteriacea* (SRP) species complex, provide an interesting model to address these questions. SRP pathogens belong to three genera, *Pectobacterium, Dickeya* and *Musicola*, of the family *Pectobacteriacea* within the order *Enterobacteral*. Taxonomic studies recognize 38 species within the SRP group, of which 23 belong to the genus *Pectobacterium*, 12 belong to the *Dickeya* genus and 2 were formerly assigned to the *Dickeya* genus and now belong to the newly described genus *Musicola* (Charkowski 2018; Hugouvieux-Cotte-Pattat et al. 2021). All SRP attack the host plant by secreting a cocktail of plant cell wall degrading enzymes through the type 2 secretion system (T2SS), resulting in rotting and maceration of plant tissues on which the bacteria actively develop (Charkowski 2018; Hugouvieux-Cotte-Pattat et al. 2014). Due to their collective large host spectrum, SRP plant infections lead to severe economic losses and are collectively recognized as one of the ten most important bacterial plant pathogens (Mansfield et al. 2012; Ma et al. 2007; Portier et al. 2020). Among SRP species, some species like *Pectobacterium brasiliense*, *Pectobacterium carotovorum* or *Pectobacterium versatile* are described as broad range species isolated from a large number of plant species while other like *Pectobacterium parmentieri*, *Pectobacterium atrosepticum* or *Dickeya solani* have been mainly recorded on a single host (Ma et al. 2007; Portier et al. 2020; Hugouvieux-Cotte-Pattat et al. 2023). *P. versatile* is the most frequently isolated taxon among the SRP species, both on plants and in the environment, a characteristic that might be linked with its higher resistance to antibiotics than

other *Pectobacterium* spp. (Royer et al. 2022; Smoktunowicz et al. 2022; Ben Moussa et al. 2022; Portier et al. 2020) but this species is currently considered as a minor pathogen not responsible for severe outbreaks but frequent companion species during disease or on symptomless plants (Curland et al. 2021; Ma et al. 2022; Smoktunowicz et al. 2022). Some newly described species like *Pectobacterium aquaticum* or *Pectobacterium quasiaquaticum* have been isolated solely from river water and their potential host plants (if any) are currently unknown raising the possibility that these species act are merely saprophytes on plant debris or evolved toward hosts alternative to plant, for example as gut species of plant feeding insect or water microfauna (Pédron et al. 2019; Ben Moussa et al. 2022, 2023). Species belonging to the *Dickeya* genus are well known to infect ornamentals of high economical value but several species could also be observed on major crops such as maize (*Dickeya zeae*) rice (*Dickeya oryzae*) or potato (*Dickeya dianthicola* or *D. solani*) where they have been responsible of severe outbreaks (Hugouvieux-Cotte-Pattat et al. 2023).

Potato production, estimated according to FAO to over 376 million tons worldwide in 2021, is particularly exposed to SRP species. In potato field, SRP triggers a disease called blackleg. This name referred to the necrosis observed at the steam basis of infected potato plant. Harvested potato tubers could also develop a severe rotting, called soft rot, that could destroy the whole harvest. Given its economic importance, potato is the most intensively surveyed crop attacked by SRP and 15 different SRP species have been recorded on potato worldwide (Toth et al. 2021). In Europe and North America, *P. atrosepticum* was initially considered to be the primary pathogen causing blackleg and soft rot in potatoes. However, from the 1970s, *D. dianthicola* increased in prevalence, until the appearance of *D. solani* in the early 2000s while more recently the spread of *P. parmentieri*, and *P. brasiliense* was observed (van der Wolf et al. 2021). The succession of these prevalent species is not yet understood. Notably, aggressivity of the species is likely not the main factor explaining the prevalence of species in potato field (de Werra et al. 2021). Other traits such as survival ability in the environment or competition/cooperation abilities within the host plant are likely involved in the observed turn over. Importantly, mix of SRP spp. during infection could represent up to 20% of recorded symptoms (Ge et al. 2021; Motyka-Pomagruk et al. 2021; de Werra et al. 2021). These mixed infections probably contribute to the evolution of epidemic clones through HGT transfer of trait associated to the bacterial fitness (Khayi et al. 2015; Royer et al. 2022). Furthermore latent mix of SRP spp. are also reported on asymptomatic potato tuber and could represent up to 18% detected latent infection (Degefu 2021; Smoktunowicz et al. 2022). These latent infections likely influence the

102 dynamic of disease through cooperation and competition but this has not been investigated in
103 details.
104 The aim of the present work was to experimentally assess the fate of mix infection. To
105 understand the dynamic of coinfections, we set up 16 different synthetic communities of 6 SRP
106 strains to mimic coinfection. Bacteria present in each synthetic community were representative
107 of 2 different species, with 3 strains per species. These communities were inoculated on potato
108 tuber or on growth medium and the outcome of each synthetic community was followed by
109 amplification and Illumina sequencing of the discriminative housekeeping gene *gap*A (Cigna
110 et al. 2017; Ben Moussa et al. 2022). We also compared disease rating and bacterial
111 multiplication on potato tuber during coinfection and single species infection. Overall, the
112 results indicate that competition, cooperation and trophic interactions shape the bacterial SRP
113 community and allow for the maintenance of SRP diversity.
114
115 **Materials and Methods**
116
117 **Strains and media used**
118 The strain used in this study are described in table S1. The bacterial media used were LB
119 medium without NaCl (hereafter LB: per liter 10 g tryptone, 5 g yeast extract) and TSB (per
120 liter: 1,7 g casein peptone, 0.3 g soya peptone, 0.3 g NaCl, 0.25 g dipotassium hydrogen
121 phosphate, 0.25 g glucose). When needed, 15 g agar per liter were added for solid media.
122
123 **Inocula preparation**
124 The bacteria were plated on LB plates and incubated overnight at 28°C. A single colony was
125 then used to inoculate 2 ml of LB medium which was incubated overnight at 28°C, with
126 agitation at 120 rpm. This liquid culture (100 µl) was used to inoculate a 10% TSB agar plate,
127 which was incubated overnight at 28°C. The grown bacterial layer was then suspended in 50
128 mM phosphate buffer (pH 7) and adjusted to an DO_{600nm}=1. The 3 strains of the same species
129 were then mixed in a 1/1/1 ratio. An exception was the inoculum composed of *P. parvum* (2
130 strains) and *P. polaris* (1 strain), which were mixed together as the experiment was set up before
131 the description of the *P. parvum* species, a close relative of *P. polaris* (Pasanen et al. 2020).
132 The bacterial load of each 3 strains-mixtures was check by serial dilution and plating on TSB
133 agar plates. The species mixtures were then prepared by mixing two of the prepared strain-
134 mixtures in volumes 1/1. Each final species-mixture is thus the mixture of 6 strains adjusted to
135 DO_{600nm}=1 in the ratio 1/1/1/1/1/1, where the first strain-mixture corresponds to one of the nine

136 following species: *P. atrosepticum, P. carotovorum, P. parmentieri, P. versatile, P.*
137 *polaris/P.parvum, D. dianthicola, D. solani, P. versatile, P. aquaticum*, and the second strain-
138 mixture corresponds either to the species *P. aquaticum* or to the species *P. versatile*. A 2 ml
139 aliquot of each time zero species-mix inoculum was stored at -20°C until DNA extraction.
140 These 18 species-mixtures were then used to inoculate triplicates of 2 ml TSB liquid medium
141 (1 µl in 2 ml) or 10 potato tubers (10 µl per tuber). The inoculated TSB medium was incubated
142 at 26°C with shaking during 48h. Serial dilution and plating was performed to check the
143 bacterial growth at the end of the culture. The bacterial load at time zero (inoculum) and at the
144 end of the experiment were used to calculate the number of bacterial generation achieved ($\log_{10}$
145 (cfu end experiment/cfu T0)/$\log_{10}$ (2)). Cultures were then centrifuged and the pellet was kept
146 at -20°C until DNA extraction.
147
148 **In vitro bacterial competition assays**
149 Pairwise in vitro bacterial competition assays were performed between the *P. brasiliense, P.*
150 *versatile* and *P. aquaticum* strains (3 strains per species, 81 combinations tested). Briefly,
151 overnight TSB cultures of each strain were adjusted to an DO_{600nm} = 0.15. Samples of 5 µl of
152 the strain 1 were spotted onto freshly poured agar lawn inoculated with strain 2 (1 ml with 15
153 ml TSB agar medium) and plates were allowed to grow for 24 h at 28°C. If strain 1 inhibits the
154 growth of strain 2, a clear halo is observed around the spot of strain 1. Experiment was repeated
155 twice with similar results.
156
157 **Potato inoculation**
158 Three experiments were performed, the first one was devoted to analyze the mono-species
159 infection with the mix of the 3 strains/species. The second and third one involved mix of two
160 different species (6 strains) with either *P. aquaticum* species or *P. versatile* species challenged
161 by one of the other 8 species.
162 For each mix, 10 potato tubers were thoroughly washed, and surface disinfected in a 1 %
163 hypochlorite solution bath prior inoculation and each tuber was punctured with pipette tips
164 containing 10 µl of the inoculum. The tip was left in the tuber. As a negative control, a pipette
165 tip with 10µl sterile water was inserted into one tuber. Inoculated tubers were placed on paper
166 towel in plastic boxes and 50 mL of distilled water was poured into the bottom of the boxes and
167 the boxes were carefully closed to achieve relative humidity above 90 %. After 5 days of
168 incubation at 26°C, the tubers were cut and the entire macerating symptom was collected and
169 weighed. Part of the symptom (50 to 300 mg) was also weighed and suspended in 1 ml of sterile

170 phosphate buffer in order to count by serial dilution and plating the bacterial load present in the
171 symptom. To recover the bacteria within the symptoms, the rest of the symptom was suspended
172 with 7 ml of 50 mM phosphate buffer and stirred for 4 hours at ambient temperature. The tubes
173 were then left without shaking for 10 minutes to allow the excess starch to settle and 2 ml at the
174 surface of the suspension was recovered and centrifuged for 10 minutes at 10,000 g. The formed
175 pellet was kept at -80°C until DNA extraction.
176
177 **Statistical analysis**
178 One specie mix (*P. aquaticum/P. versatile*) was shared between the second and the third
179 experiments and this allowed to eliminate inter-experiment variation unrelated to the involved
180 species mix before statistical analysis. To do so we corrected the maceration weight observed
181 in the third experiment with the following coefficient X = (mean of *P. aquaticum/P.versatile*
182 10 potato tubers maceration weight of the 2ndexperiment)/ mean of *P. aquaticum/P.versatile* 10
183 potato tubers maceration weight results of the 3rd experiment) before statistical analysis.
184 Statistical analyses were performed in R version 4.0.2 using a Kruskal-Wallis test with p-value
185 < 0.05 followed by a post-hoc test (Dunn test with Bonferroni correction). Spearman correlation
186 calculation were performed on line (https://biostatgv.sentiweb.fr/?module=tests/spearman).
187
188 **DNA extraction, DNA amplification and sequencing**
189 For each of the 18 species-mix analyzed, DNA extraction was performed on 10 ml of the time
190 zero inoculum, on 2 ml of each of the TSB triplicate after 48h of culture and on 2 ml of 3 to 6
191 potato macerated tubers symptoms. The bacteria were pelleted by centrifugation and DNA
192 extraction was performed with the Wizard® genomic DNA purification kit (Promega).
193 Amplification and sequencing were performed at MR DNA (www.mrdnalab.com, Shallowater,
194 TX, USA). Briefly, the *gap*A 376 partial gene sequence was amplified using PCR primers
195 *gap*AF376: GCCCGTCTCACAAAGA and *gap*AR: TCRTACCARGAAACCAGTT) with
196 barcode on the forward primer. PCR using the HotStarTaq Plus Master Mix Kit (Qiagen, USA)
197 was performed under the following conditions: 94°C for 3 min, followed by 28 cycles of 94°C
198 for 30 s, 57°C for 40 s and 72°C for 1 min, after which a final elongation step at 72°C for 5 min
199 was performed. Amplified PCR products were checked in 2 % agarose gel to determine the
200 success of amplification and the relative intensity of bands. Multiple samples were pooled
201 together in equal proportions based on their molecular weight and DNA concentrations. Pooled
202 samples were purified using calibrated Ampure XP beads and used to prepare Illumina DNA
203 library. Sequencing was performed on a MiSeq sequencer following the manufacturer's

204 guidelines. Sequence data were processed using MR DNA analysis pipeline (MR DNA,
205 Shallowater, TX, USA). In summary, sequences were joined, depleted of barcodes and
206 sequences <150bp or with ambiguous base calls were removed. Reads were filtered based on
207 Q score and expected error probability and any read with a number of expected errors greater
208 than 1.0 were discarded.

209

210 **Illumina sequencing analysis**

211 After quality trimming, a total of 2,230,817 and 3,215,158 reads were obtained for *in vitro*
212 (TSB, 64 samples) and potato tuber (100 samples) assays respectively, with an average of
213 34,857 ± 963 and 32,152 ± 7538 reads per samples respectively.
214 In order to quantify the distribution of the *Pectobacterium* and *Dickeya* strains after *in vitro*
215 growth or potato inoculation, reads were aligned to the corresponding amplified sequences of
216 the *gap*A gene, using the nucleotide-nucleotide Blastn tool (version 2.11.0+, e-value threshold
217 10^{-5}). Only reads with 100% full-length identity were used (547,866 reads, 24.6% of the total
218 reads and 1,213,517 reads, 37.7% of the total reads for *in vitro* and potato tuber assays
219 respectively. A few potato tubers were withdrawn of the analysis since unexpected *P.*
220 *parmentieri* sequences were observed, suggesting an initial presence of this pathogen as latent
221 species hosted on the tuber prior to the inoculation.

222 Bacterial distribution analysis was performed at the species level for all assays (sum of all
223 strains of the same species), and at the strain level when it was possible. In fact, for some
224 species, certain strains cannot be distinguished due to sequence similarities: *P. versatile*
225 CFBP6051 and A73.1, all *D. dianthicola* strains, all *D. solani* strains, *P. parmentieri* CFBP1338
226 and CFBP5382, *P. atrosepticum* CFBP1527 and CFBP1453, *P. carotovorum* CFBP6074 and
227 CFBP1402, all *D. polaris* strains.

228

229 **Model presentation**

230 The equations of the model are:

231 $dDX/dt = k(D_R - D_X) - (gA - \epsilon)D_X X + cX/z + X$

232 $dDA/dt = k(D_R - D_A) - g_A D_A A$

233 $dDR/dt = -k(2D_R - D_X - D_A) - \lambda D_R$

234 $dX/dt = (g_A - \epsilon)\, D_X X - mX$

235 $dA/dt = g_A D_A A - mA$

236 with X the density of the species that produces enzymes able to degrade the substrate, A the

density of the cheater species that only consumes the degraded substrate without being able to produce it, D_X is the concentration of degraded substrate in the vicinity of species X (i.e. local pool of degraded substrate of X), D_A is the corresponding local substrate pool for A, and D_R is the concentration of degraded substrate in the regional environmental (hereafter regional pool of degraded substrate), k is the diffusion rate of degraded substrate between local and regional pools, c the maximum rate of enzymatic substrate degradation, z half-saturation constant of enzymatic substrate degradation, gA consumption rate of degraded substrate without cost, ϵ cost of enzyme PCWDEs production and secretion on consumption rate of degraded substrate, m Mortality rate of X and A, λ Loss of degraded substrate from regional pool. The mathematical analysis of the model together with the parameter's values used in numerical simulations are provided in supplementary file S1.

Search for carbapenem synthesis and resistance

The beta-lactam carbapenem is synthesized and degraded by the *car*ABCDEF genes while the *car*GHR genes are involved in resistance to the produced carbapenem (Shyntum et al. 2019). These genes were blast searched with *car*ABCDEFGHR genes of *P. brasiliense* CFBP6617 as query among the 27 strains used to build up the synthetic communities using the genoscope Microbial Genome Annotation & Analysis Platform (https://mage.genoscope.cns.fr/microscope/).

Results:

Set up of the experiment

A general view of the experimental set up is shown in Figure 1. Briefly, each synthetic SRP community was a mixture of two species with three strains per species. The species involved were 8 species commonly isolated from potato tubers, *P. versatile, P. atrosepticum, P. carotovorum, P. parmentieri, P. polaris, P. brasiliense, D. solani, D. dianthicola*, and one species *P. aquaticum* that was only isolated from fresh surface water. Synthetic communities were set up with either *P. versatile* or *P. aquaticum* facing one of the others 8 species. *P. versatile* and *P. aquaticum* were chosen as challenging species because of their very different distribution aera. *P. versatile* that occurs on many different plants, is the main SRP species represented in bacterial collections and is also frequently isolated from non-host environments, such as surface freshwater highlighting its ecological success among SRP (Portier et al. 2019;

Ben Moussa et al. 2022). In contrast, *P. aquaticum* has not been isolated from plants and is frequently isolated from water (Portier et al. 2020; Ben Moussa et al. 2022). SRP communities were inoculated on TSB medium or on potato tubers and the proportion of each species at the beginning and end of the experiment was assessed by Illumina sequencing of the *gap*A discriminative gene marker (Cigna et al. 2017; Ben Moussa et al. 2022). Symptoms occurring on potato tubers were also recorded for each 6 strains community and compared with symptoms observed with the mix of 3 strains of single-species inoculation.

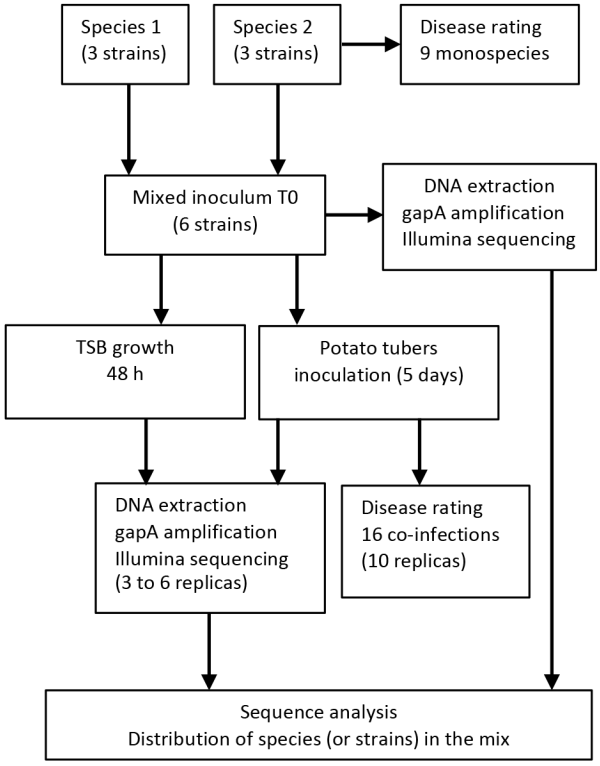

Figure 1: Set up of the experiment.

Symptoms observation and bacterial multiplication in potato tubers

Single-species infection resulted in various symptom development in potato tubers depending on the inoculated species tested. Outliers were frequently observed and there was considerable variability in response between the 10 inoculated potato tubers (Fig. 2A). The 10 potato tubers inoculated with *P. aquaticum* showed hardly any symptoms and statistical analysis confirmed that *P. aquaticum* developed less severe symptoms than *P. versatile, P. parmentieri, P. brasiliense* and *P. atrosepticum* (Fig. 2A). Bacterial multiplication was assessed and the number of bacterial generations achieved within each inoculated tuber was calculated (Fig. 2B). It varied from 0.9 to 13.7 with a median of 8.9 depending on the tuber inoculated. This

multiplication rate correlated with the weight of macerating symptoms (Spearman correlation 0.451, p-value 8.87E-14). After inoculation with *P. aquaticum*, bacterial multiplication within the tubers was much lower than with other single inoculated single species, confirming *P. aquaticum* poor ability to rot potato tuber (Fig. 2B) as already described (Ben Moussa et al, 2023). The addition of either *P. versatile* or *P. aquaticum* to the inoculation mix did not affect the severity of the symptoms observed compared to the other single species inoculation but *P. aquaticum* (Fig. 2A). Bacterial multiplication was also unaffected by the mixed-species inoculation (Fig. 2B). In the following experiments 3 to 6 tubers from each SRP community were analyzed by amplification and Illumina sequencing of the *gap*A barcode.

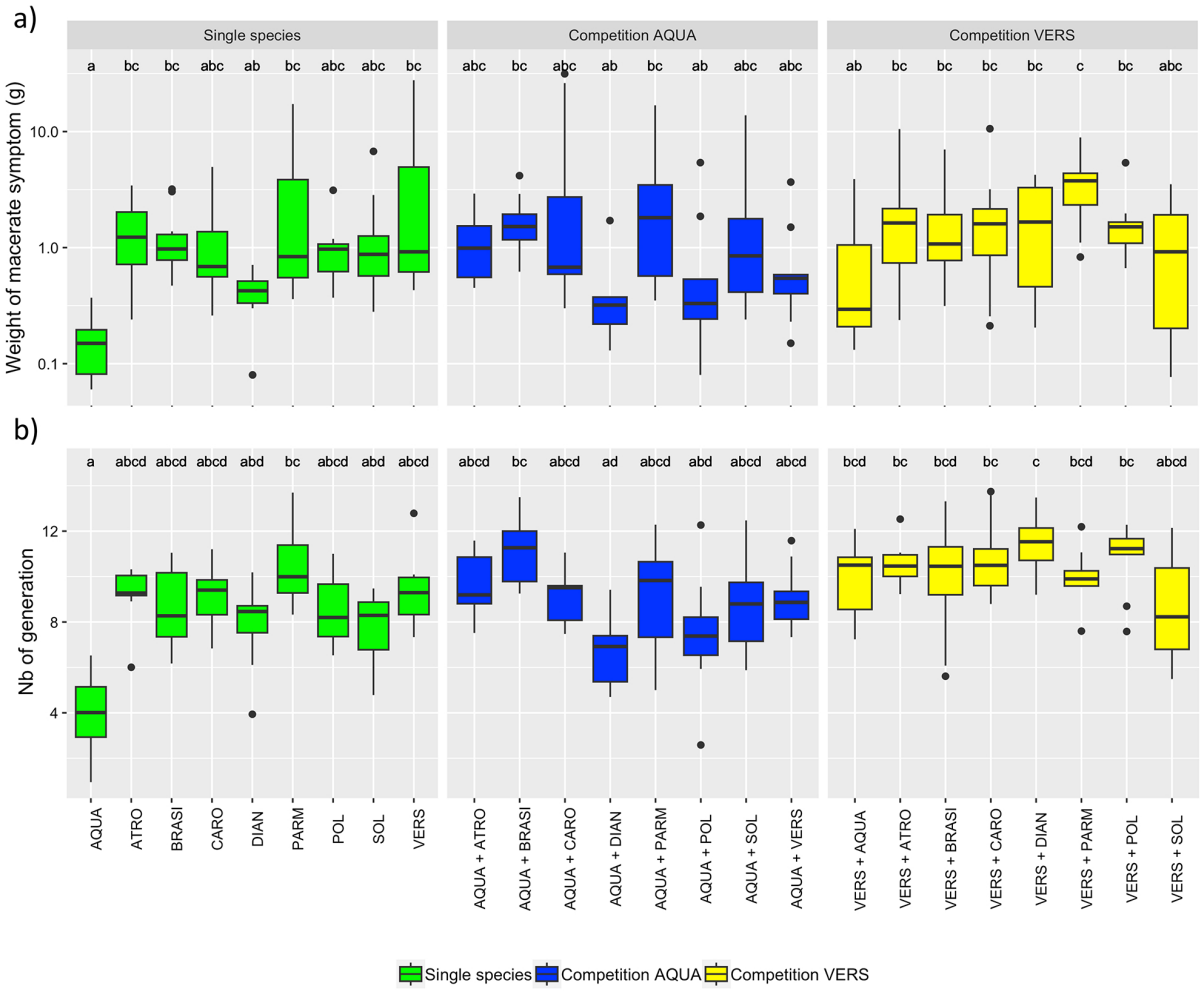

Figure 2: Symptoms and bacterial growth of the SRP synthetic communities on potato tubers. a) Weight of macerate symptom b) bacterial growth within potato tuber. Single-species mixtures (3 strains) are shown in green. Two-species mixtures (6 strains) are shown in blue and yellow for *P. aquaticum*, and *P. versatile* consortia respectively. AQUA : *P. aquaticum* ; ATRO: *P. atrosepticum ;* BRASI: *P. brasiliense* ; CARO: *P. carotovorum*; PARM: *P. parmentieri* ; POL: *P.*

306 *polaris* ; SOL: *D. solani*; VERS: *P. versatile* . The result of the statistical analysis is represented by the
307 letters (a, b, c) at the top of the boxplots. The bacterial mixtures sharing the same letter(s) are not
308 statistically different from each other (P>0.05 Kruskal Wallis followed by Dunn test with the Bonferroni
309 correction). The strains used in each bacterial mixture are listed in Table S1.
310

311 **Species outcome within SRP communities inoculated in TSB medium**

312 Bacterial multiplication was assessed after 48 hours of growth on TSB medium and the number
313 of bacterial generations obtained was calculated. It ranged from 4.2 to 9 generations and was
314 repeatedly higher in the mixture containing *P. aquaticum* compared to the mixture containing
315 *P. versatile* (Fig. S1). A total of 2,230,817 sequences were obtained after Illumina sequencing,
316 with an average of 34,857 ± 963 sequences per sample. The 376 pb *gapA* sequence allowed us
317 to distinguish all the inoculated species and to calculate the percentage of sequences assigned
318 to *P. aquaticum* or *P. versatile* within each SRP community at time zero and after 48 hours of
319 growth (Fig 3 A and B). At time zero, *P. aquaticum* or *P. versatile* represented 30% to 60% of
320 the inoculum in each mix containing another *Pectobacterium* species as expected for an even
321 inoculation of each strain. However, in the SRP community containing *Dickeya spp.*, *P.*
322 *aquaticum* and *P. versatile* made up more than 60% of the mixture. This deviation was
323 particularly important for the mix containing *D. dianthicola* as *P. versatile* and *P. aquaticum*
324 represented 78% and 79% respectively. A similar deviation was observed after counting the cfu
325 of each individual 3 species mix at time zero indicative of a higher inoculation of *P. versatile*
326 and *P. aquaticum* compared to the *D. dianthicola* species in the initial mix (data not shown).
327 This bias is likely due to the fact that *D. dianthicola* is highly mucoid impacting the optical
328 density-cfu relation.
329 After 48 hours of growth, with an average number of generations of 6.7 after 48 hours of
330 growth, the initial population size represents only around 1% of the final population size. The
331 *gap*A barcode allowed to analyzed the proportion of each SRP species within the synthetic
332 community (Fig. 3 A and B). *P. aquaticum* and *P. versatile* were considered to drastically
333 outcompete the other SRP species if the mean percentage for the three replicates reached at
334 least 90% at the end of the experiment. They were considered to be drastically outcompeted by
335 the other SRP species if their mean percentage for the three replicate was inferior to 10%.
336 Finally, if the mean percentage of *P. aquaticum* or *P. versatile* was between 10% and 90%, *P.*
337 *aquaticum* and *P. versatile* were considered to be coexisting with their challenging SRP species.
338 Using this criterion most of the SRP community (12 out of 16) allowed coexistence of both
339 species after 2 days of growth in TSB medium (Fig. 3A and B). *P. aquaticum* outcompeted *D.*

340 *dianthicola* and coexisted with all the other challenging species. *P. versatile* was outcompeted
341 when co-inoculated with *P. brasiliense, P. carotovorum* or *D. solani* and it coexisted with the
342 other species at various levels.
343

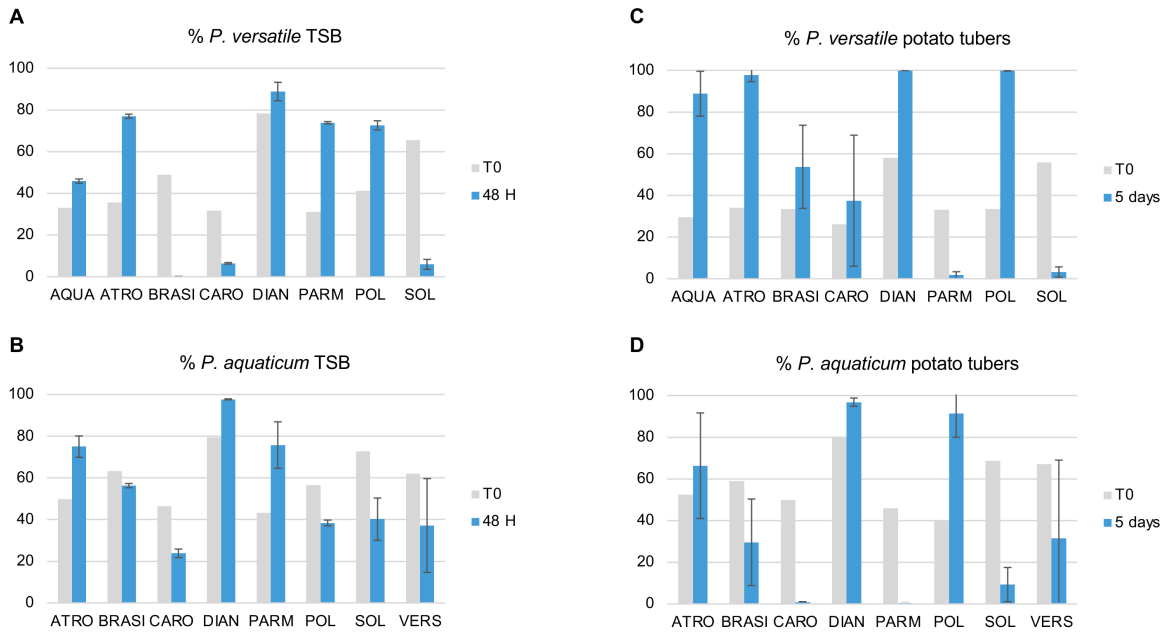

344

345 **Figure 3:** Species outcome within SRP communities.
346 Percentage of *P. versatile* or *P. aquaticum* in mixed-species SRP communities after 48h TSB growth (A
347 and B) or 5 days post inoculation within potato tuber (C and D). Grey bars: % of *P. aquaticum* or *P.*
348 *versatile* within the inocula at time zero, Blue: bars % of *P. aquaticum* or *P. versatile* after 48 hours
349 growth in TSB or 5 days within potato tubers. Three replicates were analysed after 48h growth in TSB
350 and 3 to 5 potato tubers were analysed 5 days post inoculation. Bars : standard deviation. Species's
351 acronym: AQUA : *P. aquaticum* ; ATRO: *P. atrosepticum ;* BRASI: *P. brasiliense* ; CARO: *P.*
352 *carotovorum*; PARM: *P. parmentieri* ; POL: *P. polaris* ; SOL: *D. solani*; VERS: *P. versatile.*
353

354 **Species outcome within SRP communities inoculated within potato tubers**

355 A total of 3,215,158 sequences were obtained after Illumina sequencing, with an average of
356 32,152 ± 7538 sequences per sample. We calculated the percentage of reads assigned to *P.*
357 *aquaticum* or *P. versatile* in the mixed-species SRP communities at time zero and after growth
358 inside the potato tubers (Fig. 3 C and D). Using the same criteria as after TSB growth,
359 coexistence was observed 5 days post infection in 6 out of the 16 mixed-species SRP
360 communities inoculated in potato tubers. Within potato tubers, *P. aquaticum* was outcompeted
361 in presence of *P. carotovorum, P. parmentieri* and *D. solani*, it outcompeted *D. dianthicola* and
362 *P. polaris* and coexisted with *P. atrosepticum, P. brasiliense* and *P. versatile*. *P. versatile* was

363 outcompeted in the presence of *P. parmentieri* and *D. solani*, it outcompeted *P. atrosepticum,*
364 *D. dianticola* and *P.polaris/P.parvum* and coexisted with *P. aquaticum, P. brasiliense and P.*
365 *carotovorum*.
366 The outcome of the competitions in potato tubers was different from that observed after growth
367 on TSB for 10 out of the 16 SRP communities tested (Table 1). For example, within potato
368 tubers *P. aquaticum* was outcompeted by *P. carotovorum, P. parmentieri* and *D. solani* while
369 it coexisted with each of these three species in TSB. Similarly, while *P. versatile* coexisted with
370 *P. brasiliense* and *P. carotovorum* in potato tubers, it was outcompeted by both species in the
371 TSB medium. As well, *P. aquaticum* and *P. versatile* were outcompeted by *P. parmentieri* in
372 potato tubers but both species coexisted with *P. parmentieri* in the TSB medium. Overall, for
373 the 16 tested combinations, coexistence between the two species twice was more frequent in
374 TSB medium (12/16 SRP community tested) than within potato tuber (6/16 SRP community
375 tested).
376
377 **Table 1:** Comparison of species outcome after growth in TSB or potato tuber.

Species mix	Potato tuber	TSB
AQUA-ATRO	65.02	75
AQUA-BRASI	29.57	56.28
AQUA-CARO	0.77	23.8
AQUA-DIAN	96.81	94.88
AQUA-PARM	0.32	75.76
AQUA-POL	91.37	38.39
AQUA-SOL	9.29	40.21
AQUA VERS	38.29	37.14
VERS-ATRO	97.64	77.02
VERS-BRASI	53.72	0.13
VERS-CARO	37.44	6.42
VERS-DIAN	99.94	88.87
VERS-PARM	1.72	73.89
VERS-POL	99.81	72.64
VERS-SOL	3.23	5.93
VERS-AQUA	88.8	45.88

378
379 Blue: coexistence. Green: *P. versatile or P. aquaticum* dominates. Red: *P. versatile* or *P. aquaticum* was
380 outcompeted. The number indicated the % mean of *P. aquaticum* or *P. versatile* at the end of the
381 experiment
382

Modelling of cheater persistence

The SRP species *P. aquaticu*m has been isolated from water and is not recorded on plant (Pédron et al. 2019; Portier et al. 2020). We noticed here the poor capacity of the *P. aquaticum* strains to rot potato tuber and to multiply within symptoms (Fig. 2), a phenotypic trait that was already described previously (Ben Moussa et al. 2023). We observed nevertheless, that *P. aquaticum* when co-inoculated with another species, could be maintained and even become dominant in several synthetic communities tested (Fig. 3C and D). To investigate the potential mechanisms by which *P. aquaticum* might persist when co-inoculated with other species and become even dominant, we analysed a model describing the dynamics of two species in competition for one common resource originating from the degradation of a substrate by the enzymatic activity of only one of the two species (species X, Fig. 4A, Appendix model). The other species (A) is a cheater as it does not contribute to the production of degraded substrate, and thus has no cost related to enzyme production in that context. The model considers heterogeneous distribution of the degraded substrate, with specific concentrations in the vicinity of each species (species local pool of degraded substrate, Fig. 4A) resulting from the depletion of degraded substrate through consumption for both species X and A, and from the creation of degraded substrate by enzyme production for species X. Degraded substrate diffuses at a given rate between the two species-specific local pools and a regional pool, determining the interactions between the species A and X through their indirect effect on the concentration of degraded substrate in the regional pool. The analysis of the model (Fig. 4 B and C, supplementary file S1) suggests that the cheater species A can persist when it has sufficiently higher growth rate than the producer species X (i.e. sufficient cost of enzyme production on the growth rate of species X) and when species X is sufficiently efficient in producing degraded substrate (i.e. high maximum rate of substrate degradation). Higher diffusion rate of degraded substrate between the local and regional pools also favours species A persistence for lower enzyme production cost of species X (Fig. 4B and C). The cheater species can become dominant (i.e. proportion of abundance of A higher than 0.5) when A has significantly higher growth rate than X (intermediate to high cost of enzyme production) and when the rate of substrate degradation by X is high, especially when the diffusion of degraded substrate in the environment are high. However, in such cases the abundance of X is low (see supplementary file S1) and we are at the limit of the coexistence domain between X and A. Indeed, as A has relatively very high growth rate in comparison to X, this can lead to the exclusion of X by A through competition for the consumption of degraded substrate, further leading to the extinction of A due to the loss of production of degraded substrate by X (see supplementary file S1).

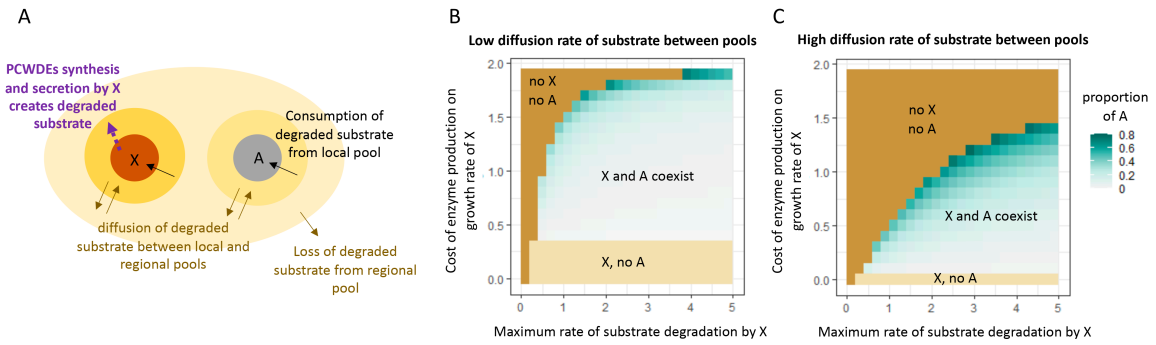

Figure 4: Modeling of cheater abundance.

A: Schematic description of the model analysing the coexistence between a species X that produces degraded substrate and a cheater species A that only consumes such substrate. The producer species X and its local pool of degraded substrate are represented by a brown circle and a dark yellow circle respectively. The cheater species A and its local pool are represented by a grey and a light-yellow circle respectively. The oval shape corresponds to the regional pool of degraded substrate in the environment. B and C: effects of the rate of substrate production and the cost of degradation for X on coexistence and relative abundance of A for two scenarios of flows of degraded substrate in the environment.

Strains outcome within the SRP communities

Beyond the species level, the 376 pb *gap*A Illumina sequenced fragment allowed the differentiation of the 3 inoculated strains of *P. brasiliense* or *P. aquaticum* and one of the three strains for *P. versatile*, *P. carotovorum*, *P. parmentieri* and *P. atrosepticum* (Table S2). This allowed us to analyze the fate of these 10 strains within the 16 tested SRP communities within potato tubers or TSB (Table 2, Fig. S2 and S3). Comparison of the fate of these 10 strains showed that the outcome was mainly determined at the strain level (Fig. 4, see Fig. S2, Fig. S3 for the 32 tested combinations). In 20 cases, within the 3 strains of a single species, the fate of the 3 strains was different. For example, within the *P. aquaticum/P. brasiliense* community in which the six strains could be distinguished, after growth in TSB, one strain belonging to the *P. aquaticum* species (A212) and two strains belonging to the *P. brasiliense* species (CFBP5381 and CFBP3230) were outcompeted, while two strains of *P. aquaticum* (A101 and A127) and one strain of *P. brasiliense* (CFBP6617) coexisted (Fig. 5). The result of the same community grown on potatoes was different, allowing the coexistence of one *P. brasiliense* strain (CFBP6617) and only one *P. aquaticum* strain (A101) (Fig. 5). Also, within the *P. aquaticum/P. parmentieri* community, the *P. parmentieri* strain CFBP8475 outcompeted the 5 other strains on potato tubers, but this was not the case on TSB (Fig. 5).

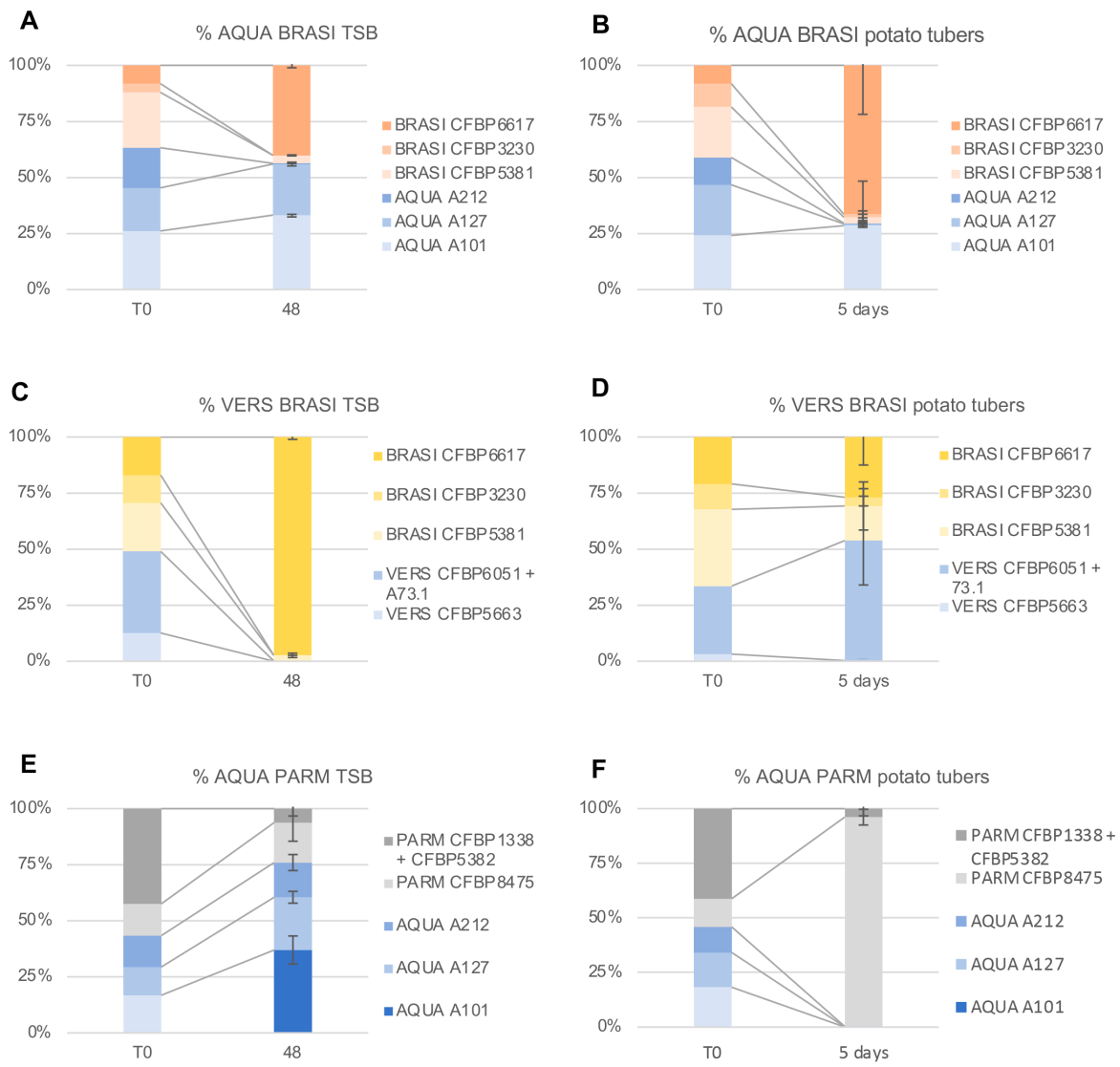

Figure 5: Examples of strains outcome within SRP communities.

The proportion of each strain in 3 different mixed-species SRP communities after 48h growth in TSB growth or 5 days post inoculation within potato tubers is indicated in the legend of each graph. *P. aquaticum-P. brasiliense* strains consortium in TSB (A) or within potato tuber (B) *P. versatile* - *P. brasiliense* strains consortium in TSB (C) or within potato tuber (D). *P. aquaticum* - *P. parmentieri* strains consortium in TSB (E) or within potato tuber (F). In each grap the first column represents the % of each strain within the inoculum (T0), the second column represents the outcome of the inoculated community after 48h in TSB or 5 days post potato tubers inoculation. Three replicates were analysed after 48h growth in TSB and 3 to 5 potato tubers were analysed 5 days post inoculation. Bars: standard deviation. Species's acronym: AQUA : *P. aquaticum* ; ATRO: *P. atrosepticum ;* BRASI: *P. brasiliense* ; CARO: *P. carotovorum*; PARM: *P. parmentieri* ; POL: *P. polaris* ; SOL: *D. solani*; VERS: *P. versatile.* The names of each strain follow the species'names.

458 The outcome of each strain was different between potato tubers and TSB, and overall, the
459 outcompeted strains were more numerous within the potato tuber (72%) than after growth on
460 TSB (32%) (Table 2).
461
462 **Table 2:** Outcome of individual strains within the tested SRP communities.

Single strain discriminated with the gapA barcode	nb of tested combination	potato tubers			TSB		
		>90%	<10%	10-90%	>90%	<10%	10-90%
VERS CFBP5663	9	0	9	0	0	3	6
AQUA A101	9	0	4	5	0	0	9
AQUA A127	9	0	8	1	0	2	7
AQUA A212	9	0	7	2	0	4	5
ATRO CFBP7375	2	0	1	1	0	2	0
BRASI CFBP5381	2	0	1	1	0	2	0
BRASI CFBP3230	2	0	2	0	0	2	0
BRASI CFBP6617	2	0	2	0	1	0	1
CARO CFBP2046	2	0	2	0	0	1	1
PARM CFBP8475	2	1	0	1	0	0	2
Total	48	1	36	11	1	16	31
%		2%	72%	22%	2%	32%	62%

463
464 VERS: *P. versatile*; AQUA: *P. aquaticum*; ATRO: *P. atrospecticum*; BRASI: *P. brasiliense*; CARO:
465 *P. carotovorum*; PARM: *P. parmentieri*.
466
467 However, the dominance of a single strain over the 5 other strains of the SRP community was
468 rarely observed both within tubers and in TSB medium: only *P. parmentieri* dominates in potato
469 tubers when associated with *P. aquaticum* and, in TSB medium, *P. brasiliense* dominates when
470 associated with *P. versatile* (Table 2, Fig. 5). In the other synthetic communities tested, on TSB
471 or within the potato tubers, coexistence of at least two strains was observed in 23 of the 32
472 combinations tested, the remaining 7 combinations were inconclusive because we could not
473 differentiate some strains with the *gap*A barcode (Fig. S2 and S3).
474
475 **Focus on the SRP communities involving *P. brasiliense***
476 The strain *P. brasiliense* CFBP6617, also called 1692, is a model strain known to produce,
477 among other toxic compounds, a carbapenem antibiotic (Holden et al. 1998; Shyntum et al.
478 2019). We set up pairwise *in vitro* competition assays between the 6 strains of *P. brasiliense*
479 and *P. aquaticum* to check for carbapenem production. This showed that the *P. brasiliense*

strain CFBP6617 inhibited the growth of the other two *P. brasiliense* strains, CFBP3220 and CFBP5381, and of the two *P. aquaticum* strains, A212 and A127 (Fig. 6). The *P. aquaticum* strain A101 was not inhibited by the *P. brasiliense* strain CFBP6617. Consistent with this latter result, the *car*G, *car*H and *car*F genes conferring resistance to carbapenem (Coulthurst et al. 2005) were only detected in the genome of the strain *P. aquaticum* A101. During our pairwise inhibition tests, we also observed that the *P. aquaticum* strain A127 produces an unknown compound that inhibits the growth of the strain *P. brasiliense* CFBP6617. The radius of action of this unknown toxin is smaller than the one induced by the carbapenem production by the *P. brasiliense* strain CFBP6617 (Fig. 6).

A

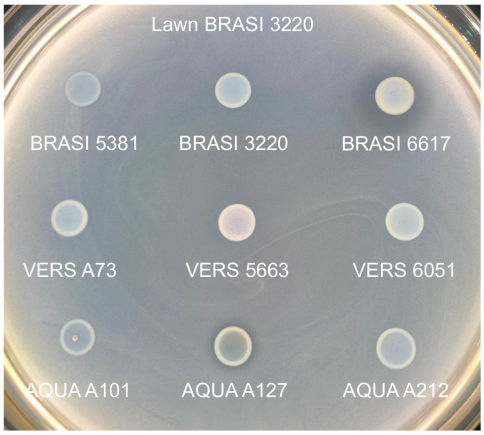

B

		Spot	
	strain	BRASI 6617	AQUA A127
Lawn	BRASI 6617	R	s
	BRASI 3220	S	s
	BRASI 5381	S	s
	VERS 6051	R	s
	VERS 5663	R	R
	VERS A73	R	s
	AQUA A212	S	R
	AQUA A127	S	R
	AQUA A101	R	R

Figure 6: Pairwise competition assays.

Pairwise competition assays were setup between the 9 strains belonging to the species *P. brasiliense*, *P. aquaticum* and *P. versatile*. A: example of inhibition assay showing that the *P. brasiliense* strain CFBP3230 (lawn BRASI 3220) is inhibited by the *P. brasiliense* strain CFBP6617 (spot BRASI 6617) and also by the *P. aquaticum* strain A127 (spot AQUA A127). Note that the radius of inhibition triggered by the *P. aquaticum* strain A127 is smaller than the one triggered by the *P. brasiliense* strain CFBP6617. B: inhibition observed for the 81 pairwise tested competitions. R: no inhibition; S: the strain in the lawn

is inhibited by the strain in the spot with a large radius of inhibition; s: the strain in the lawn is inhibited by the strain in the spot with a small radius of inhibition; BRASI: strains belonging to the *P. brasiliense* species; AQUA: strains belonging to the *P. aquaticum* species; VERS: strains belonging to *the P. versatile* species.

These observed pairwise inhibitions could probably explain the outcome of the *P. aquaticum/P. brasiliense* community after growth on TSB medium (Fig. 5), as the 3 strains CFBP 6617, A127 and A101 were efficiently maintained after growth on this medium, while the 3 other strains were outcompeted. The result of the same community on potato tubers was slightly different as only 2 strains, CFBP6617 and A101, were efficiently maintained (Fig. 5). This could probably be explained by the fact that the unknown toxic compound that counteract the growth of *P. brasiliense* strain CFBP6617 is not produced by strain A127 or inefficient within potato tuber, while the carbapenem is still produced within potato tuber. Surprisingly, within the *P. versatile/P. brasiliense* community, we observed that the *P. brasiliense* strain CFBP5381 was maintained within the potato tuber despite its sensitivity to the carbapenem produced by the *P. brasiliense* strain CFBP6617 (as revealed with the *P.aquaticum/P. brasiliense* SRP community) (Fig. 5). This suggests that at least one of the two *P. versatile* strains CFBP6051 or A73 still observed in the potato tubers at the end of the experiment is interfering with the toxic effect of *P. brasiliense* CFBP6617 to allow the growth of *P. brasiliense* CFBP5381. The mechanism that allows the *P. versatile* strains to resist to carbapenem toxicity of *P. brasiliense* CFBP6617 is unknown, as the two strains do not carry the carbapenem resistance genes *car*G, *car*H and *car*F in their genomes. Whatever the mechanism involved, it is either not induced or not efficient in TSB medium, as CFBP6617 dominates over the other 5 strains of the *P.brasiliense/P. versatile* community TSB medium.

Discussion:

The dynamic of bacterial microbial communities is an important research field. Theoretical studies showed that cooperative trophic interaction generally leads to the steady coexistence of distinct bacterial species, that organize themselves to create a community-level metabolism that best exploits the nutrients present (Gralka et al. 2020; Taillefumier et al. 2017). This is exemplified by synthetic metabolic consortia set up for various biotechnological applications that regroup highly diverse bacteria with different metabolic capacity that could be stably maintained. As well, metabolic cross feeding could allow maintenance of bacterial species

531 otherwise outcompeted in natural environment (Franza et al, 2016). The maintenance of
532 microbial diversity within pathogenic bacterial species complex cannot follow the same rule as,
533 in that case, the microbes within these species complex are closely phylogenetically related
534 with highly similar metabolic properties. This metabolic closeness implies a strong substrate
535 overlap likely associated with strong competition between species within the same niche (Weiss
536 et al. 2022). It is therefore not straightforward to understand which mechanisms allow the
537 maintenance of diversity within these pathogenic species complexes. The bacterial SRP species
538 complex is probably one of the most diverse species complexes of plant pathogenic bacteria. It
539 gathers 38 accepted or proposed species and at least 15 SRP species have been identified on the
540 potato host, with frequent co-infection with at least 2 species (Toth et al. 2021). The work
541 presented here takes advantage of *gap*A barcoding Illumina sequencing to analyze the bacterial
542 dynamics of 16 different synthetic SRP communities involving 6 strains belonging to two
543 different species.
544 The outcome of the 16 synthetic communities was highly dependent on environmental
545 conditions and strongly differed between potato tubers and TSB stirred liquid medium. The
546 striking outcome differences of the synthetic community in the two different environments
547 should warns us on the use of synthetic liquid medium to test consortia stability when these
548 consortia should be used in a different environment. Notably, coexistence between the two
549 species was twice more frequent in TSB liquid medium than within potato tubers and
550 outcompeted strains were more numerous within the potato tubers than after growth on TSB
551 liquid medium. Competition through production of secreted toxic compounds, such as
552 carbapenem (Coulthurst et al. 2005; McGowan et al. 1997), carotovoricin (Nguyen et al. 1999;
553 Itoh et al. 1978), bacteriocins (Chuang et al. 2007; Chan et al. 2011; Roh et al. 2010; Grinter et
554 al. 2012), NRPS-PKS secondary metabolites (Brual et al. 2023; Cheng et al. 2013) have been
555 described in SRP. The production of many of these compounds is enhanced by plant extracts
556 or in potato tubers (Bellieny-Rabelo et al. 2019; Mattinen et al. 2007) and this could explain
557 that more strains are outcompeted during growth in potato tubers. Furthermore, competition
558 mechanisms relying on cell to cell contact, like the type 6 secretion system (T6SS), are also
559 described in SRP (Shyntum et al. 2019; Arizala and Arif 2019) but are likely inefficient in liquid
560 stirred medium. Modelling studies showed that in a structured environment such as that found
561 in potato tubers, the production of antimicrobial molecules could be beneficial even if the
562 producer is rare (Chao and Levin, 1981; Durrett and Levin, 1997; Gardner et al., 2004). The
563 enhanced production of antimicrobial molecules and their higher efficiency within a structured

environment, such as potato tubers, likely explain the higher competition observed within potato tubers compared to liquid TSB medium.

Our results also illustrate that this competition is strain-specific rather than species-specific, as in many combinations we observed that the fate of the 3 strains of the same species was different. This is likely related to the fact that toxin production and toxin resistance are functional traits associated with strains rather than with species and are generally encoded within the accessory genomes of each species, as exemplified here by biosynthesis and resistance to carbapenem (Shyntum et al. 2019). In most combinations, the *P. brasiliense* strain CFBP6617 outcompeted the other two *P. brasiliense* strains, consistent with the observed pairwise *in vitro* competition and the presence of the carbapenem cluster in the strain genomes. However, within the *P. versatile/P. brasiliense* synthetic community, we observed an interference towards the toxic effect of *P. brasiliense* CFBP6617 on *P. brasiliense* strain CFBP5381, likely mediated by *P. versatile* strains. This interference may involve the secreted β-lactamase commonly found in *P. versatile* strains which may inactivates the carbapenem antibiotic (Royer et al. 2022). Further work is needed to test this hypothesis. *In vitro* pairwise inhibition indicated that "face-to-face" competition may also occur in some of the synthetic SRP communities tested, as for example *P. brasiliense* strain CFBP6617 is toxic to *P. aquaticum* strain A127, but the reverse is also true. The complexity of the competitive interplay between strains is enhanced by the number of toxic compounds and resistance mechanisms known to be produced by SRP. Theoretical models highlight that chemical warfare between microbes promote diversity (Kelsic et al. 2015; Czárán et al. 2002). The fact that each SRP strains carries its own set of toxic compounds and resistance mechanisms could therefore contribute to the maintenance of multiple strains as observed with the majority of the 16 synthetic communities tested. The complexity of the competition between SRP strains rather than species probably also explains the temporal and spatial succession of different SRP species in epidemic outbreaks.

Beyond the competition mechanisms, the virulence factors of SRP may also contribute to the maintenance of SRP diversity, as the main virulence factors of SRP, i.e. the ability of SRP to degrade the plant cell wall through the secretion of PCWDEs, can be considered as a public good used to feed the whole community. In potato tubers, the important release of nutrients once SRP express their main virulence factors allows the development of associated commensals (Kõiv et al. 2015). Here, we observed that *P. aquaticum* strains were efficiently maintained in the population within potato tubers in 5 out of 8 synthetic communities tested. We also observed that *P. aquaticum* strains were unable to produce soft rot disease symptoms

598 and to multiply efficiently in the potato tubers when inoculated alone. The inability of *P.*
599 *aquaticum* strains to produce soft rot symptoms when inoculated alone strongly suggests that
600 the T2SS and associated virulence factors are not properly induced within the potato tuber and,
601 as such, *P. aquaticum* does not share the cost of producing virulence factors. However, when
602 mixed with other species, *P. aquaticum* strains could eventually become dominant, suggesting
603 that they can behave as cheaters, benefiting greatly from nutrient sharing. Several independent
604 mechanisms could be proposed to explain this efficient cheating behavior. Firstly, the low
605 expression of T2SS and the associated virulence factors and the smaller genome of *P.*
606 *aquaticum* strains compared to that of other SRP species may allow a more rapid multiplication
607 at the expense of the other SRP species. In support of this hypothesis, we observed here that in
608 TSB medium the 8 synthetic communities with *P. aquaticum* have a tendency to grow at higher
609 density in TSB medium than the 8 synthetic communities with *P. versatile*. It has also been
610 reported that *P. aquaticum* strains have increased mobility compared to that of other SRP
611 species (Ben Moussa et al. 2023). This may also influence the ability of *P. aquaticum* strains to
612 access nutrients within the symptoms. *P. aquaticum* has never been isolated from potatoes in
613 the field or in storage, and their cheating behavior observed here could therefore be considered
614 an artefact. Nevertheless, the observation of this cheating behavior suggests that other SRP
615 species could also behave as cheaters in the field, as plants infected with several SRP species
616 are often observed. This is supported by the fact that the repertoire and regulation of virulence
617 factors is variable among SRP species (Babujee et al. 2012; Jonkheer et al. 2021; Arizala and
618 Arif 2019; Li et al. 2018), likely allowing for a trade-off between growth and the ability to
619 cheat. Interestingly, our modelling suggests that the more efficient the SRP strain is at
620 decomposing potato tubers, the higher the abundance of the cheaters in the symptoms. This
621 greater abundance of the cheaters may affect the ability to detect the SRP strain responsible for
622 the symptoms and increase the risk of not identifying the initial SRP strain responsible for the
623 epidemic. Therefore, field sampling plans should be calibrated to account for this risk.
624 In summary, the dynamics of the 16 synthetic SRP communities presented here highlight some
625 possible mechanisms allowing both the maintenance of high SRP diversity within the SRP
626 species complex and the regular species shifts responsible for outbreaks observed in the field.
627 Cooperation for virulence, exemplified by cheating behavior of *P. aquaticum*, and the
628 complexity of competition between strains, are two mechanisms that likely contribute to the
629 maintenance of the SRP complex diversity. The fact that competition occurs at the strain level
630 rather than the species level probably also explains the regular appearance of new species
631 responsible for epidemic outbreaks. This suggests that deep sequencing or *gap*A barcoding of

plant symptoms are important to understand epidemic dynamic and rapidly identify new strains responsible for outbreaks in the field.

Authors contributions

Jacques Pédron: Conceptualization (equal); supervision (equal): data curation (lead): formal analysis (equal), methodology (equal), visualization (equal), writing original draft (equal), writing-review and editing (equal)

Christelle Gomes de Faria: investigation (equal), writing-review and editing (equal)

Sylvia Thieffry: Methodology (equal), conceptualization (equal), writing-review and editing (equal)

Elisa Thebault: Supervision (equal), conceptualization (lead), methodology (equal), visualization (equal), writing-review and editing (equal).

Marie-anne Barny: Funding acquisition (lead), supervision (equal), investigation (equal), visualization (equal), writing original draft (equal), writing-review and editing (equal)

Acknowledgements:

We thank Denis Faure and Jérémy Cigna for helpful discussions during the setup of the experiment. We also thank Angel Alfon for performing the pairwise competition tests and Hajar Ben Moussa for statistical analysis and vizualisation of Fig. 2. This work was possible due to funding contract ANR-17-CE32-0004.

Conflict of interest statement

The authors declare they have no conflict of interest relating to the content of this article.

Data, script and code availability

Supplemental data are available in the tables S1 and S2, the figures S1, S2, S3 and the file S1 for model details. Sequenced data and the script used to analyse the sequences. could be found in the zenodo file DOI 10.5281/zenodo.10212828 (https://zenodo.org/records/10212829).

References:

1. Arizala, D., and Arif, M. 2019. Genome-wide analyses revealed remarkable heterogeneity in pathogenicity determinants, antimicrobial compounds, and CRISPR-Cas systems of complex phytopathogenic genus *Pectobacterium*. Pathogens. 8:247. DOI: 10.3390/pathogens8040247
2. Babujee, L., Apodaca, J., Balakrishnan, V., Liss, P., Kiley, P. J., Charkowski, A. O., et al. 2012. Evolution of the metabolic and regulatory networks associated with oxygen availability in two phytopathogenic enterobacteria. BMC Genomics. 13:110. DOI:10.1186/1471-2164-13-110
3. Bellieny-Rabelo, D., Tanui, C. K., Miguel, N., Kwenda, S., Shyntum, D. Y., and Moleleki, L. N. 2019. Transcriptome and comparative genomics analyses reveal new functional insights on key determinants of pathogenesis and interbacterial competition in *Pectobacterium* and *Dickeya* spp. Appl. Environ. Microbiol. 85 DOI: 10.1128/AEM.02050-18
4. Ben Moussa, H., Bertrand, C., Rochelle-Newall, E., Fiorini, S., Pédron, J., and Barny, M.-A. 2022. The diversity of soft rot *Pectobacteriaceae* along the Durance river stream in the south-east of France revealed by multiple seasonal surveys. Phytopathology DOI : 10.1094/PHYTO-12-21-0515-R
5. Ben Moussa, H., Pédron, J., Hugouvieux-Cotte-Pattat, N., and Barny, M. 2023. Two species with a peculiar evolution within the genus *Pectobacterium* suggest adaptation to a new environmental niche. Environ. Microbiol. :1462-2920.16479. DOI: 10.1111/1462-2920.16479
6. Brual, T., Effantin, G., Baltenneck, J., Attaiech, L., Grosbois, C., Royer, M., et al. 2023. A natural single nucleotide mutation in the small regulatory RNA ArcZ of *Dickeya solani* switches off the antimicrobial activities against yeast and bacteria ed. Pascale Romby. PLOS Genet. 19:e1010725. DOI: 0.1371/journal.pgen.1010725
7. Chan, Y.-C., Wu, J.-L., Wu, H.-P., Tzeng, K.-C., and Chuang, D.-Y. 2011. Cloning, purification, and functional characterization of Carocin S2, a ribonuclease bacteriocin produced by *Pectobacterium carotovorum*. BMC Microbiol. 11:99.DOI: 10.1186/1471-2180-11-99
8. Charkowski, A. O. 2018. The changing face of bacterial soft-rot diseases. Annu. Rev. Phytopathol. 56:269–288.DOI: 10.1146/annurev-phyto-080417-045906
9. Cheng, Y., Liu, X., An, S., Chang, C., Zou, Y., Huang, L., et al. 2013. A nonribosomal peptide synthase containing a stand-alone condensation domain is essential for phytotoxin

695 zeamine biosynthesis. Mol. Plant-Microbe Interactions. 26:1294–1301. DOI:
696 10.1094/MPMI-04-13-0098-R
697 10. Chuang, D., Chien, Y., and Wu, H.-P. 2007. Cloning and expression of the *Erwinia*
698 *carotovora* subsp. *carotovora* gene encoding the low-molecular-weight bacteriocin Carocin
699 S1. J. Bacteriol. 189:620–626. DOI: 10.1128/JB.01090-06
700 11. Cigna, J., Dewaegeneire, P., Beury, A., Gobert, V., and Faure, D. 2017. A gapA PCR-
701 sequencing assay for identifying the *Dickeya* and *Pectobacterium* potato pathogens. Plant
702 Dis. 101:1278–1282. DOI: 10.1094/PDIS-12-16-1810-RE
703 12. Coulthurst, S. J., Barnard, A. M. L., and Salmond, G. P. C. 2005. Regulation and
704 biosynthesis of carbapenem antibiotics in bacteria. Nat. Rev. Microbiol. 3:295–306. DOI:
705 10.1038/nrmicro1128
706 13. Curland, R. D., Mainello, A., Perry, K. L., Hao, J., Charkowski, A. O., Bull, C. T., et al.
707 2021. Species of *Dickeya* and *Pectobacterium* isolated during an outbreak of blackleg and
708 soft rot of potato in northeastern and north central United States. Microorganisms.
709 9:1733.DOI: 10.3390/microorganisms9081733
710 14. Czárán, T. L., Hoekstra, R. F., and Pagie, L. 2002. Chemical warfare between microbes
711 promotes biodiversity. Proc. Natl. Acad. Sci. 99:786–790.DOI: 0.1073/pnas.01239989
712 15. Degefu, Y. 2021. Co-occurrence of latent *Dickeya* and *Pectobacterium* species in potato
713 seed tuber samples from northern Finland. Agric. Food Sci. DOI:10.23986/afsci.101446
714 16. Ge, T., Ekbataniamiri, F., Johnson, S. B., Larkin, R. P., and Hao, J. 2021. Interaction
715 between *Dickeya dianthicola* and *Pectobacterium parmentieri* in potato infection under field
716 conditions. Microorganisms. 9:316.DOI: 10.3390/microorganisms9020316
717 17. Gralka, M., Szabo, R., Stocker, R., and Cordero, O. X. 2020. Trophic interactions and
718 the drivers of microbial community assembly. Curr. Biol. 30:R1176–R1188.DOI:
719 10.1016/j.cub.2020.08.007
720 18. Grinter, R., Milner, J., and Walker, D. 2012. Ferredoxin containing bacteriocins suggest
721 a novel mechanism of iron uptake in *Pectobacterium* spp ed. Pierre Cornelis. PLoS ONE.
722 7:e33033.DOI: 10.1371/journal.pone.0033033
723 19. Holden, M. T. G., McGowan, S. J., Bycroft, B. W., Stewart, G. S. A. B., Williams, P.,
724 and Salmond, G. P. C. 1998. Cryptic carbapenem antibiotic production genes are widespread
725 in *Erwinia carotovora*: facile trans activation by the carR transcriptional regulator.
726 Microbiology. 144:1495–1508. DOI: 10.1099/00221287-144-6-1495
727 20. Hugouvieux-Cotte-Pattat, N., des-Combes, C. J., Briolay, J., and Pritchard, L. 2021.
728 Proposal for the creation of a new genus *Musicola* gen. nov., reclassification of *Dickeya*

paradisiaca (Samson et al. 2005) as *Musicola paradisiaca* comb. nov. and description of a new species

21. *Musicola keenii* sp. nov. Int. J. Syst. Evol. Microbiol. 71 DOI: DOI: 10.1099/ijsem.0.005037

22. Hugouvieux-Cotte-Pattat, N., Condemine, G., and Shevchik, V. E. 2014. Bacterial pectate lyases, structural and functional diversity: Bacterial pectate lyases. Environ. Microbiol. Rep. 6:427–440. DOI: 10.1111/1758-2229.12166

23. Hugouvieux-Cotte-Pattat, N., Pédron, J., and Van Gijsegem, F. 2023. Insight into biodiversity of the recently rearranged genus *Dickeya*. Front. Plant Sci. 14:1168480. DOI: 10.3389/fpls.2023.1168480

24. Itoh, Y., Izaki, K., and Takahashi, H. 1978. Purification and characterization of a bacteriocin from *Erwinia carotovora*. J. Gen. Appl. Microbiol. 24:27–39.DOI: 10.2323/jgam.24.27

25. Jonkheer, E. M., Brankovics, B., Houwers, I. M., van der Wolf, J. M., Bonants, P. J. M., Vreeburg, R. A. M., et al. 2021. The *Pectobacterium* pangenome, with a focus on *Pectobacterium brasiliense,* shows a robust core and extensive exchange of genes from a shared gene pool. BMC Genomics. 22:265.DOI: 10.1186/s12864-021-07583-5

26. Kelsic, E. D., Zhao, J., Vetsigian, K., and Kishony, R. 2015. Counteraction of antibiotic production and degradation stabilizes microbial communities. Nature. 521:516–519. DOI: 10.1038/nature14485

27. Khayi, S., Blin, P., Jacques Pédron, J., Chong, T.-M., Chan, K.-G., Mohieddine Moumni, M., et al. 2015. Population genomics reveals additive and replacing horizontal gene transfers in the emerging pathogen *Dickeya solani*. BMC Genomics. 16:788. DOI: 10.1186/s12864-015-1997-z

28. Li, X., Ma, Y., Liang, S., Tian, Y., Yin, S., Xie, S., et al. 2018. Comparative genomics of 84 *Pectobacterium* genomes reveals the variations related to a pathogenic lifestyle. BMC Genomics. 19 DOI: 10.1186/s12864-018-5269-6

29. Ma, B., Hibbing, M. E., Kim, H.-S., Reedy, R. M., Yedidia, I., Breuer, J., et al. 2007. Host range and molecular phylogenies of the soft rot Enterobacterial genera *Pectobacterium* and *Dickeya*. Phytopathology. 97:1150–1163. DOI: 10.1094/PHYTO-97-9-1150

30. Ma, X., Brazil, J., Rivedal, H., Perry, K. L., Frost, K., and Swingle, B. 2022. First report of *Pectobacterium versatile* causing potato soft rot in oregon and washington. Plant Dis. 106:1292.DOI: 10.1094/PDIS-08-21-1635-PDN

31. Mansfield, J., Genin, S., Magori, S., Citovsky, V., Sriariyanum, M., Ronald, P., et al.

2012. Top 10 plant pathogenic bacteria in molecular plant pathology: Top 10 plant pathogenic bacteria. Mol. Plant Pathol. 13:614–629. DOI: 10.1111/j.1364-3703.2012.00804.x

32. Mattinen, L., Nissinen, R., Riipi, T., Kalkkinen, N., and Pirhonen, M. 2007. Host-extract induced changes in the secretome of the plant pathogenic bacterium *Pectobacterium atrosepticum* . PROTEOMICS. 7:3527–3537. DOI: 10.1002/pmic.200600759

33. McGowan, S. J., Sebaihia, M., O'Leary, S., Hardie, K. R., Williams, P., Stewart, G. S. A. B., et al. 1997. Analysis of the carbapenem gene cluster of *Erwinia carotovora* : definition of the antibiotic biosynthetic genes and evidence for a novel β-lactam resistance mechanism. Mol. Microbiol. 26:545–556. DOI:10.1046/j.1365-2958.1997.6001974.x

34. Motyka-Pomagruk, A., Zoledowska, S., Sledz, W., and Lojkowska, E. 2021. The occurrence of bacteria from different species of *Pectobacteriaceae* on seed potato plantations in Poland. Eur. J. Plant Pathol. 159:309–325. DOI:10.1007/s10658-020-02163-x

35. Nguyen, A. H., Tomita, T., Hirota, M., Sato, T., and Kamio, Y. 1999. A simple purification method and morphology and component analyses for carotovoricin Er, a phage-tail-like bacteriocin from the plant pathogen *Erwinia carotovora* Er. Biosci. Biotechnol. Biochem. 63:1360–1369. DOI: 10.1271/bbb.63.1360

36. Pasanen, M., Waleron, M., Schott, T., Cleenwerck, I., Misztak, A., Waleron, K., et al. 2020. *Pectobacterium parvum* sp. nov., having a Salmonella SPI-1-like Type III secretion system and low virulence. Int. J. Syst. Evol. Microbiol. 70:2440–2448. DOI: 10.1099/ijsem.0.004057

37. Pédron, J., Bertrand, C., Taghouti, G., Portier, P., and Barny, M.-A. 2019. *Pectobacterium aquaticum* sp. nov., isolated from waterways. Int. J. Syst. Evol. Microbiol. 69:745–751. DOI: 10.1099/ijsem.0.003229

38. Portier, P., Pédron, J., Taghouti, G., Dutrieux, C., and Barny, M.-A. 2020. Updated Taxonomy of *Pectobacterium* genus in the CIRM-CFBP bacterial collection: when newly described species reveal "old" endemic population. Microorganisms. 8:1441. DOI: 10.3390/microorganisms8091441

39. Portier, P., Pédron, J., Taghouti, G., Fischer-Le Saux, M., Caullireau, E., Bertrand, C., et al. 2019. Elevation of *Pectobacterium carotovorum* subsp. *odoriferum* to species level as *Pectobacterium odoriferum* sp. nov., proposal of *Pectobacterium brasiliense* sp. nov. and *Pectobacterium actinidiae* sp. nov., emended description of *Pectobacterium carotovorum* and description of *Pectobacterium versatile* sp. nov., isolated from streams and symptoms

797 on diverse plants. Int. J. Syst. Evol. Microbiol. 69:3207–3216. DOI: 10.1099/ijsem.0.003611
798 40. Roh, E., Park, T.-H., Kim, M., Lee, S., Ryu, S., Oh, C.-S., et al. 2010. Characterization
799 of a new bacteriocin, Carocin D, from *Pectobacterium carotovorum* subsp. *carotovorum*
800 Pcc21. Appl. Environ. Microbiol. 76:7541–7549.DOI: 10.1128/aem.03103-09
801 41. Royer, G., Dixit, Z., Pédron, J., Pierrat, G., Demontant, V., Berçot, B., et al. 2022.
802 Genetic and phenotypic study of the *Pectobacterium versatile* Beta-Lactamase, the enzyme
803 most similar to the plasmid-encoded TEM-1 ed. Christopher A. Elkins. Appl. Environ.
804 Microbiol. 88:e00220-22. DOI: 10.1128/aem.00220-22
805 42. Shyntum, D. Y., Nkomo, N. P., Shingange, N. L., Gricia, A. R., Bellieny-Rabelo, D.,
806 and Moleleki, L. N. 2019. The Impact of Type VI secretion system, bacteriocins and
807 antibiotics on bacterial competition of *Pectobacterium carotovorum* subsp. *brasiliense* and
808 the regulation of carbapenem biosynthesis by iron and the ferric-uptake regulator. Front.
809 Microbiol. 10 DOI: 10.3389/fmicb.2019.02379
810 43. Smoktunowicz, M., Jonca, J., Stachowska, A., May, M., Waleron, M. M., Waleron, M.,
811 et al. 2022. The international trade of ware vegetables and ornamental plants- an
812 underestimated risk of accelerated spreading of phytopathogenic bacteria in the era of
813 globalisation and ongoing climatic changes. Pathogens. 11:728.DOI:
814 10.3390/pathogens11070728
815 44. Taillefumier, T., Posfai, A., Meir, Y., and Wingreen, N. S. 2017. Microbial consortia at
816 steady supply. eLife. 6:e22644. DOI: 10.7554/eLife.22644
817 45. Toth, I. K., Barny, M., Brurberg, M. B., Condemine, G., Czajkowski, R., Elphinstone,
818 J. G., et al. 2021. *Pectobacterium* and *Dickeya*: environment to disease development. In
819 *Plant Diseases Caused by Dickeya and Pectobacterium Species*, eds. Frédérique Van
820 Gijsegem, Jan M. van der Wolf, and Ian K. Toth. Cham: Springer International Publishing,
821 p. 39–84. http://link.springer.com/10.1007/978-3-030-61459-1_3.
822 46. Weiss, A. S., Burrichter, A. G., Durai Raj, A. C., Von Strempel, A., Meng, C.,
823 Kleigrewe, K., et al. 2022. *In vitro* interaction network of a synthetic gut bacterial
824 community. ISME J. 16:1095–1109. DOI: 10.1038/s41396-021-01153-z
825 47. de Werra, P., Debonneville, C., Kellenberger, I., and Dupuis, B. 2021. Pathogenicity
826 and relative abundance of *Dickeya* and *Pectobacterium* species in Switzerland: an
827 epidemiological dichotomy. Microorganisms. 9:2270. DOI:
828 10.3390/microorganisms9112270
829 48. van der Wolf, J. M., Acuña, I., De Boer, S. H., Brurberg, M. B., Cahill, G., Charkowski,
830 A. O., et al. 2021. Diseases caused by *Pectobacterium* and *Dickeya* species around the world.

In *Plant Diseases Caused by Dickeya and Pectobacterium Species*, eds. Frédérique Van Gijsegem, Jan M. van der Wolf, and Ian K. Toth. Cham: Springer International Publishing, p. 215–261. http://link.springer.com/10.1007/978-3-030-61459-1_7

Supplementals:

Bacterial pathogens dynamic during multi-species infections

Marie-Anne Barny*, Sylvia Thieffry, Christelle Gomes de Faria, Elisa Thebault and Jacques Pédron

FigS1: Bacterial multiplication in TBS medium

FigS2: Result at strain level of the 16 synthetic communities after growth on TSB.

FigS3: Result at strain level of the 16 synthetic communities 5 days post inoculation on potato tubers.

File S1: supplemental modeling

Table S1: strains description

Table S2: Intra-species strain discrimination with the 341 nt gapA barcode

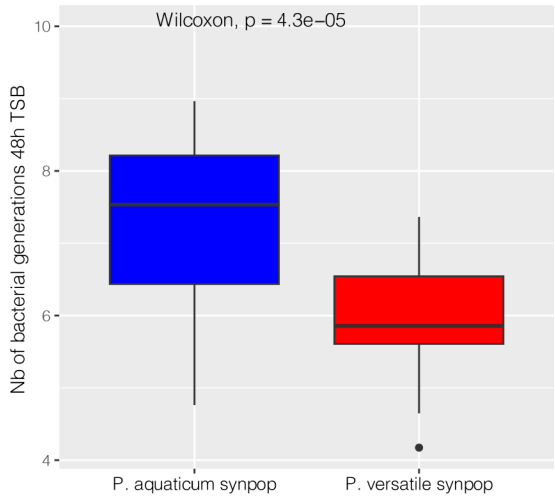

Figure S1: Bacterial multiplication in TBS medium.

For each tested communities (3 replicates), the bacterial load at time zero (inoculum) and at the end of the experiment were used to calculate the number of bacterial generation achieved ($\log_{10}$ (cfu end experiment/cfu T0)/$\log_{10}$ (2)). The *P. aquaticum* and *P. versatile* communities are compared. The result of the statistical analysis is represented by the letters (a, b) at the top of the boxplots. The bacterial mixtures sharing the same letter(s) are not statistically different from each other (P>0.05 Kruskal Wallis followed by Dunn test with the Bonferroni correction).

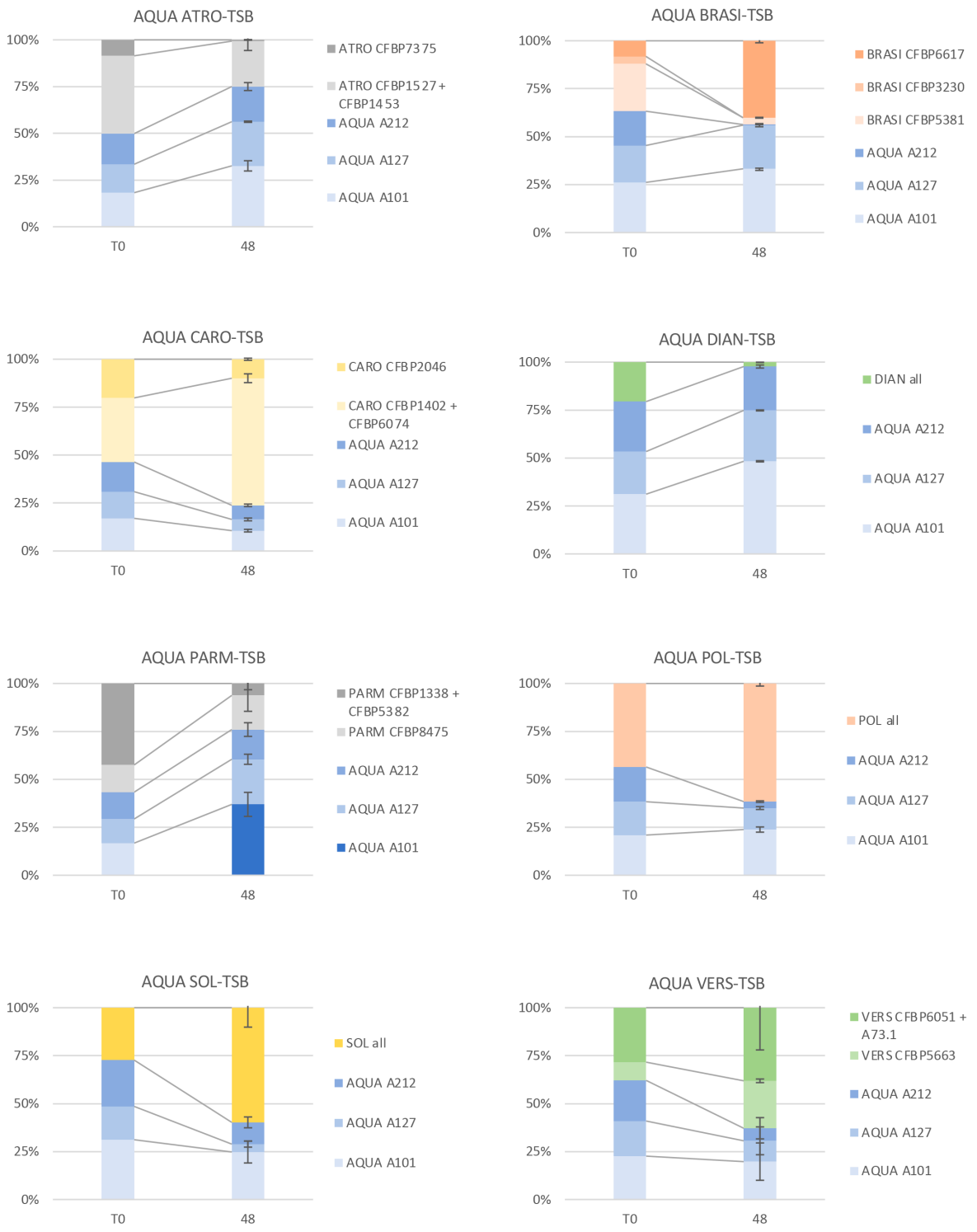
AQUA ATRO-TSB
100%
75%
50%
25%
0%
T0
48
ATRO CFBP7375
ATRO CFBP1527 + CFBP1453
AQUA A212
AQUA A127
AQUA A101
AQUA BRASI-TSB
BRASI CFBP6617
BRASI CFBP3230
BRASI CFBP5381
AQUA A212
AQUA A127
AQUA A101
AQUA CARO-TSB
CARO CFBP2046
CARO CFBP1402 + CFBP6074
AQUA A212
AQUA A127
AQUA A101
AQUA DIAN-TSB
DIAN all
AQUA A212
AQUA A127
AQUA A101
AQUA PARM-TSB
PARM CFBP1338 + CFBP5382
PARM CFBP8475
AQUA A212
AQUA A127
AQUA A101
AQUA POL-TSB
POL all
AQUA A212
AQUA A127
AQUA A101
AQUA SOL-TSB
SOL all
AQUA A212
AQUA A127
AQUA A101
AQUA VERS-TSB
VERS CFBP6051 + A73.1
VERS CFBP5663
AQUA A212
AQUA A127
AQUA A101

859

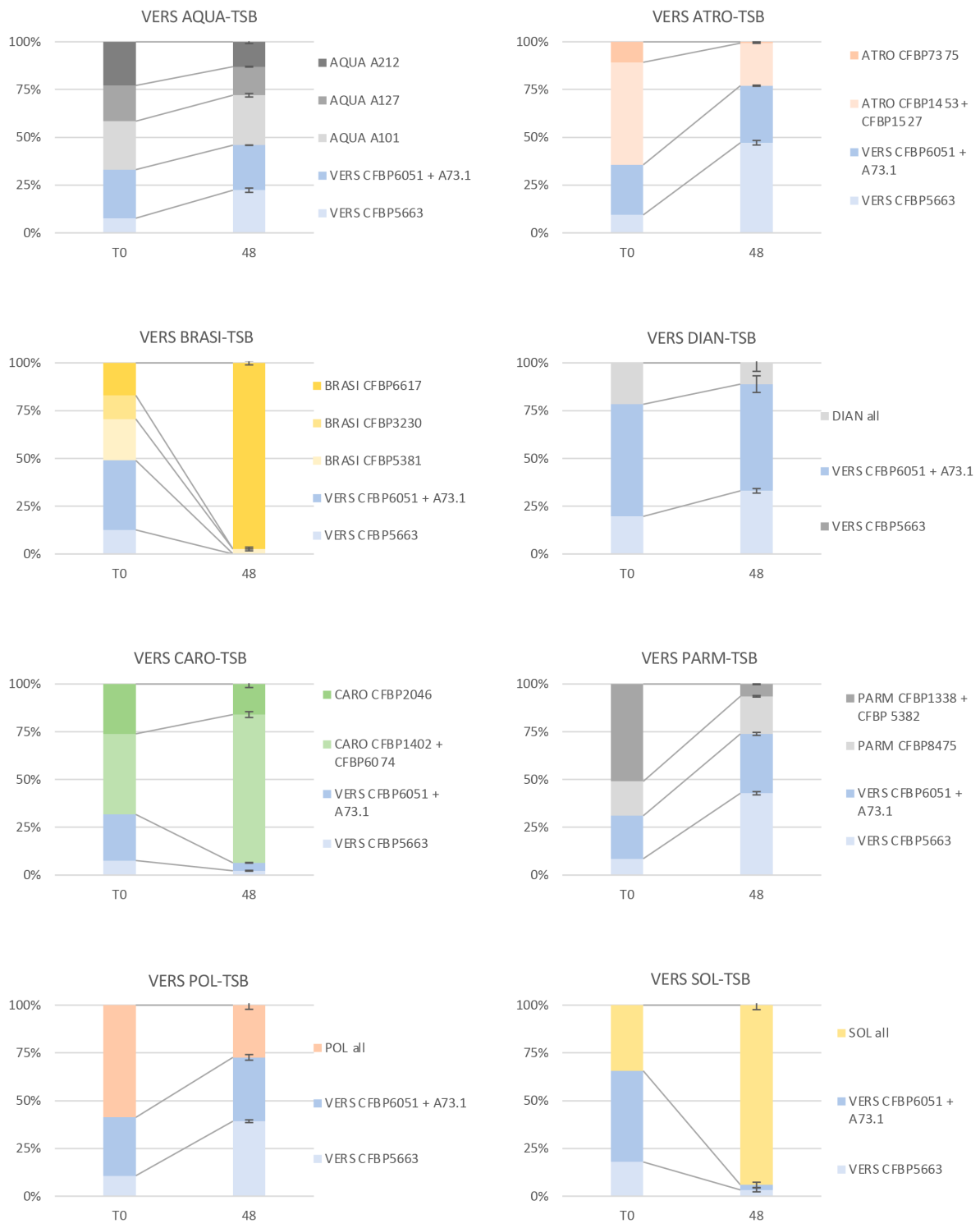

Figure S2: Result at strain level of the 16 synthetic communities after growth on TSB. The proportion of each strain (or mix of strains when strains could not be differentiated by the *gap*A barcode) is indicated in the legend of each graph. The 2 columns represent the proportion of strains observed in the inoculum (T0) and after 48h of growth in TSB medium (48) for each tested synthetic community. Error bar on the second column (48) represent the standard error observed for the 3 replicates. The 16 different tested communities are as follow: AQUA-ATRO: mix of 3 *P. aquaticum*

strains and 3 *P. atrosepticum* strains; AQUA-BRASI: mix of 3 *P. aquaticum* strains and 3 *P. brasiliense* strains; AQUA-CARO: mix of 3 *P. aquaticum* strains and 3 *P. carotovorum* strains; AQUA-DIAN: mix of 3 *P. aquaticum* strains and 3 *D. dianthicola* strains: AQUA-PARM: mix of 3 *P. aquaticum* strains and 3 *P. parmentieri* strains; AQUA-POL: mix of 3 *P. aquaticum* strains, 1 *P.polaris* and 2 *P. parvum* strains: AQUA-SOL: mix of 3 *P. aquaticum* strains and 3 *D. solani* strains, AQUA-VERS: mix of 3 *P. aquaticum* strains and 3 *P. versatile* strains; VERS-AQUA: mix of 3 *P. versatile* strains and 3 *P. aquaticum* strains; VERS-ATRO: mix of 3 *P. versatile* strains and 3 *P. atrosepticum* strains; VERS-BRASI: mix of 3 *P. versatile* strains and 3 *P. brasiliense* strains; VERS-DIAN: mix of 3 *P. versatile* strains and 3 *D. dianthicola* strains; VERS-CARO: mix of 3 *P. versatile* strains and 3 *P. carotovorum* strains; VERS-PARM: mix of 3 *P. versatile* strains and 3 *P. parmentieri* strains; VERS-POL: mix of 3 *P. versatile* strains, 1 *P. polaris* and 2 *P. parvum* strains; VERS-SOL: mix of 3 *P. versatile* strains and 3 *D. solani* strains. The strains used in each bacterial mixture are listed in Table S1.

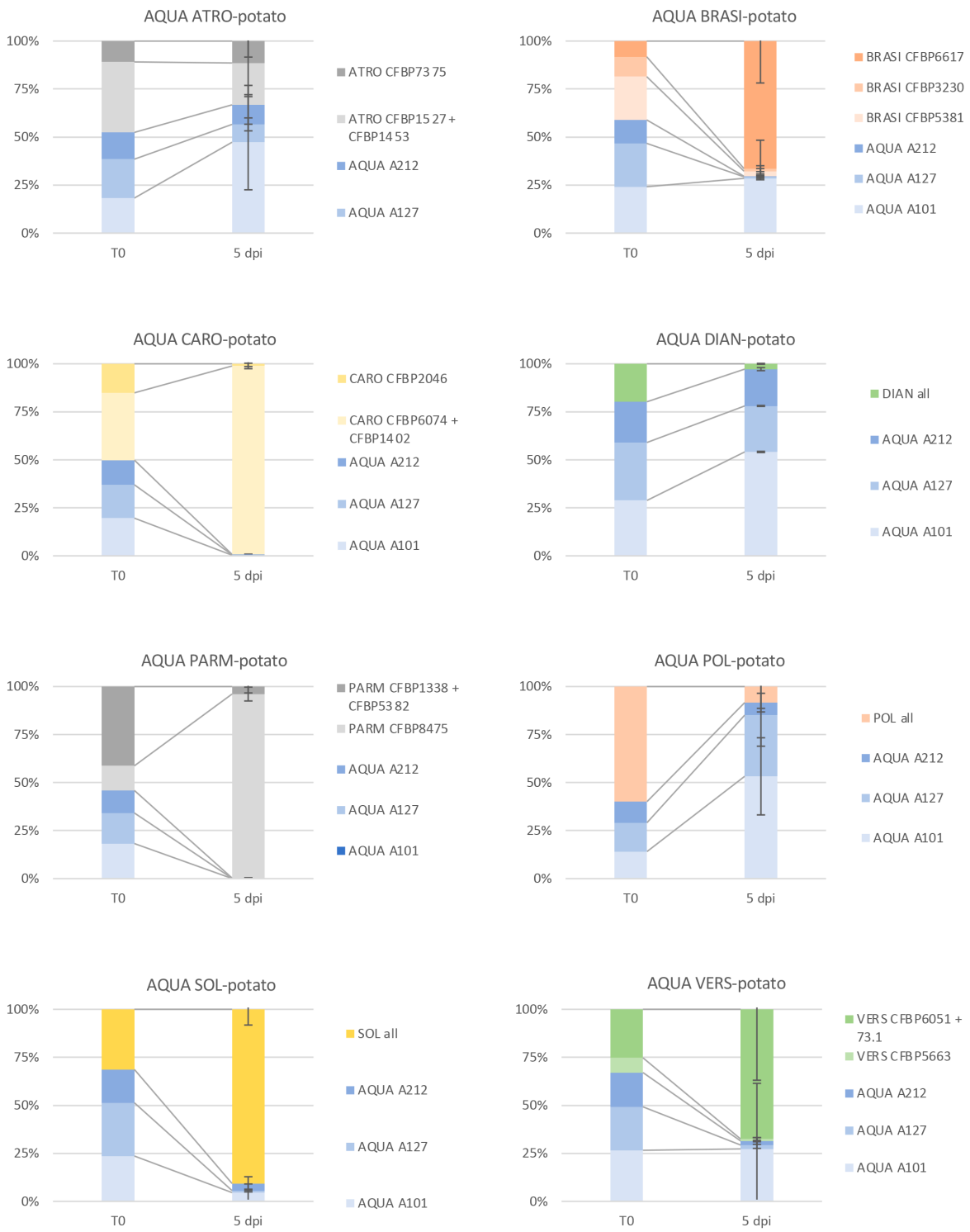
AQUA ATRO-potato
100%
75%
50%
25%
0%
T0
5 dpi
ATRO CFBP7375
ATRO CFBP1527 + CFBP1453
AQUA A212
AQUA A127
AQUA BRASI-potato
BRASI CFBP6617
BRASI CFBP3230
BRASI CFBP5381
AQUA A212
AQUA A127
AQUA A101
AQUA CARO-potato
CARO CFBP2046
CARO CFBP6074 + CFBP1402
AQUA A212
AQUA A127
AQUA A101
AQUA DIAN-potato
DIAN all
AQUA A212
AQUA A127
AQUA A101
AQUA PARM-potato
PARM CFBP1338 + CFBP5382
PARM CFBP8475
AQUA A212
AQUA A127
AQUA A101
AQUA POL-potato
POL all
AQUA A212
AQUA A127
AQUA A101
AQUA SOL-potato
SOL all
AQUA A212
AQUA A127
AQUA A101
AQUA VERS-potato
VERS CFBP6051 + 73.1
VERS CFBP5663
AQUA A212
AQUA A127
AQUA A101

880

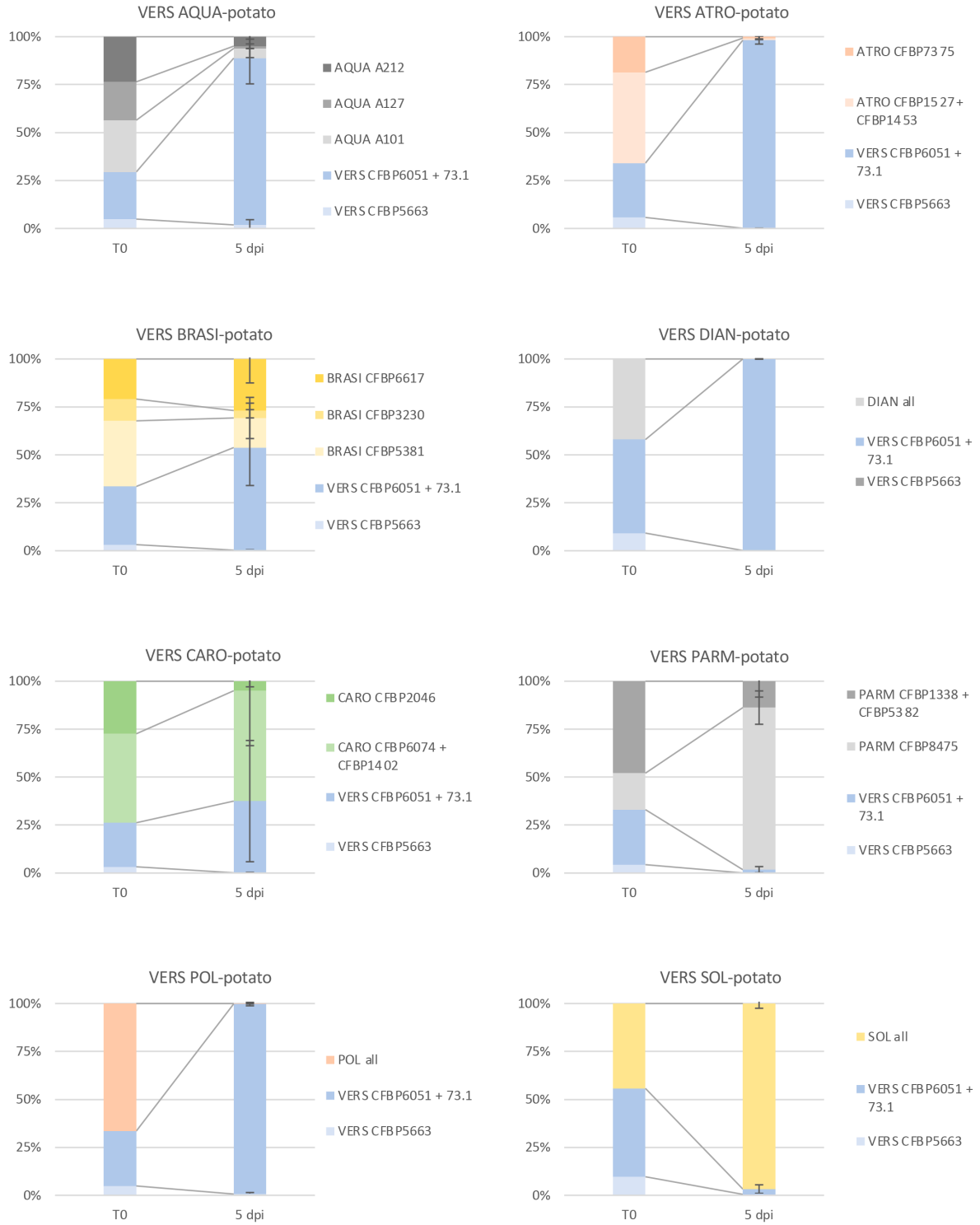

Figure S3: Result at strain level of the 16 synthetic communities 5 days post inoculation on potato tubers.

The proportion of each strain (or mix of strains when strains could not be differentiated by the *gap*A barcode) is indicated in the legend of each graph. The 2 columns represent the proportion of strains observed in the inoculum (T0) and after 5 days after inoculation within potato tubers (5 dpi) for each tested synthetic community. Error bar on the second column (5 dpi) represent the standard error observed

for the 3 to 6 inoculated potato tubers. The 16 different tested communities are as follow: AQUA-ATRO: mix of 3 *P. aquaticum* strains and 3 *P. atrosepticum* strains; AQUA-BRASI: mix of 3 *P. aquaticum* strains and 3 *P. brasiliense* strains; AQUA-CARO: mix of 3 *P. aquaticum* strains and 3 *P. carotovorum* strains; AQUA-DIAN: mix of 3 *P. aquaticum* strains and 3 *D. dianthicola* strains: AQUA-PARM: mix of 3 *P. aquaticum* strains and 3 *P. parmentieri* strains; AQUA-POL: mix of 3 *P. aquaticum* strains, 1 *P. polaris* and 2 *P. parvum* strains: AQUA-SOL: mix of 3 *P. aquaticum* strains and 3 *D. solani* strains, AQUA-VERS: mix of 3 *P. aquaticum* strains and 3 *P. versatile* strains; VERS-AQUA: mix of 3 *P. versatile* strains and 3 *P. aquaticum* strains; VERS-ATRO: mix of 3 *P. versatile* strains and 3 *P. atrosepticum* strains; VERS-BRASI: mix of 3 *P. versatile* strains and 3 *P. brasiliense* strains; VERS-DIAN: mix of 3 *P. versatile* strains and 3 *D. dianthicola* strains; VERS-CARO: mix of 3 *P. versatile* strains and 3 *P. carotovorum* strains; VERS-PARM: mix of 3 *P. versatile* strains and 3 *P. parmentieri* strains; VERS-POL: mix of 3 *P. versatile* strains, 1 *P. polaris* and 2 *P. parvum* strains; VERS-SOL: mix of 3 *P. versatile* strains and 3 *D. solani* strains. The strains used in each bacterial mixture are listed in Table S1.

File S1: supplemental modeling.

Supplementary materials for the model analyzing the coexistence between a producer of degraded substrate and a cheater

M.-A. Barny, S. Thieffry, C. Gomez de Faria, E. Thébault, J. Pédron

December 5, 2023

1 Description of the model

The equations of the model are:

$$\frac{dD_X}{dt} = k(D_R - D_X) - (g_A - \epsilon)D_X X + \frac{cX}{z + X}$$

$$\frac{dD_A}{dt} = k(D_R - D_A) - g_A D_A A$$

$$\frac{dD_R}{dt} = -k(2D_R - D_X - D_A) - \lambda D_R$$

$$\frac{dX}{dt} = (g_A - \epsilon)D_X X - mX$$

$$\frac{dA}{dt} = g_A D_A A - mA$$

with X the density of the species that produces enzymes able to degrade the substrate, A the density of the cheater species that only consumes the degraded substrate without being able to produce it, D_X is the concentration of degraded substrate in the vicinity of species X (i.e. local pool of degraded substrate of X), D_A is the corresponding local substrate pool for A, and D_R is the concentration of degraded substrate in the regional environmental (hereafter regional pool of degraded substrate). The parameters of the model are described in table 1.

Table 1: Definition of the parameters of the model and their corresponding values as used in the numerical simulations (results in the figures of main text and supplementary materials)

Parameter	Definition	Value
k	Transport rate of degraded substrate between local and regional pools	5, 50
c	Maximum rate of enzymatic substrate degradation	[0,5]
z	Half-saturation constant of enzymatic substrate degradation	1
g_A	Consumption rate of degraded substrate without cost	2
ϵ	Cost of enzyme production on consumption rate of degraded substrate	[0,1.9]
m	Mortality rate of x and A	0.1
λ	Loss of degraded substrate from regional pool	1

2 Mathematical analysis of the model

The table 2 below describes the equilibria of the model. Please note that by definition we always have $\epsilon < g_A$ (i.e. the growth rate of X in relation to the consumption of degraded substrate is always positive).

The results described in Table 1 indicate that, as expected, the cheater species A cannot persist without the producer species X. In addition, the persistence of species A requires that the cost

Table 2: The different equilibria of the model. While the equilibria could be calculated mathematically, stability was only assessed with numerical simulations and thus the details indicated in this case might not correspond to all possible cases. We have $B = k(D_R - D_X) - zm + c$ and $\Delta = B^2 - 4(g_A - \epsilon)zk(D_X - D_R) < B^2$.

Equilibrium	D_X	D_A	D_R	A	X	Feasibility conditions	Stability
No A, no X	0	0	0	0	0		yes
No A, low X	$\frac{m}{g_A-\epsilon}$	D_R	$\frac{k}{k+\lambda}D_X$	0	$\frac{B-\sqrt{\Delta}}{(g_A-\epsilon)D_X}$	$c > D_X\frac{\lambda}{\lambda+k} + zm$ $\Delta > 0$	no
No A, high X	$\frac{m}{g_A-\epsilon}$	D_R	$\frac{k}{k+\lambda}D_X$	0	$\frac{B+\sqrt{\Delta}}{(g_A-\epsilon)D_X}$	$c > D_X\frac{\lambda}{\lambda+k} + zm$ $\Delta > 0$	yes if $\epsilon < \frac{\lambda g_A}{k+\lambda}$
A, no X	D_R	$\frac{m}{g_A}$	$\frac{k}{k+\lambda}D_A$	$\frac{k(D_R-D_A)}{g_A D_A}$	0	never feasible, $A < 0$	NA
A, low X	$\frac{m}{g_A-\epsilon}$	$\frac{m}{g_A}$	$\frac{k}{k+\lambda}D_A$	$\frac{k(D_R-D_A)}{g_A D_A}$	$\frac{B-\sqrt{\Delta}}{(g_A-\epsilon)D_X}$	$\epsilon > \frac{\lambda g_A}{k+\lambda}$ (for $A > 0$) $c > zm + D_X\frac{k(k\epsilon+\lambda g_A)}{(\lambda+2k)g_A}$ $\Delta > 0$ (for $X > 0$)	no
A, high X	$\frac{m}{g_A-\epsilon}$	$\frac{m}{g_A}$	$\frac{k}{k+\lambda}D_A$	$\frac{k(D_R-D_A)}{g_A D_A}$	$\frac{B+\sqrt{\Delta}}{(g_A-\epsilon)D_X}$	$\epsilon > \frac{\lambda g_A}{k+\lambda}$ (for $A > 0$) $c > zm + D_X\frac{k(k\epsilon+\lambda g_A)}{(\lambda+2k)g_A}$ $\Delta > 0$ (for $X > 0$)	yes

sustained by X for enzyme production for the substrate degradation (ϵ) is higher than a given proportion of the maximum consumption rate of degraded substrate (g_A). The lower the transport rate k of degraded substrate between regional and local pools and the higher the loss of degraded substrate λ, the higher the cost ϵ required for the persistence of A. Meanwhile, the persistence of X with A requires that the maximum rate of substrate degradation by X (c) is higher than a threshold defined by most model parameters. In particular, this threshold increases with the cost sustained by X for enzyme production for the substrate degradation (ϵ) and with the transport rate k of degraded substrate between regional and local pools.

3 Numerical simulations of the model

To illustrate the results of the model, we calculated the equilibrium values for the range of parameters detailed in Table 1. The stability of each equilibrium was assessed by computing the eigenvalues of the Jacobian matrix at equilibrium. We also performed numerical integration of the model using the function lsoda from the R package deSolve to investigate the temporal dynamics of the two species and of the resource pools for a few study cases.

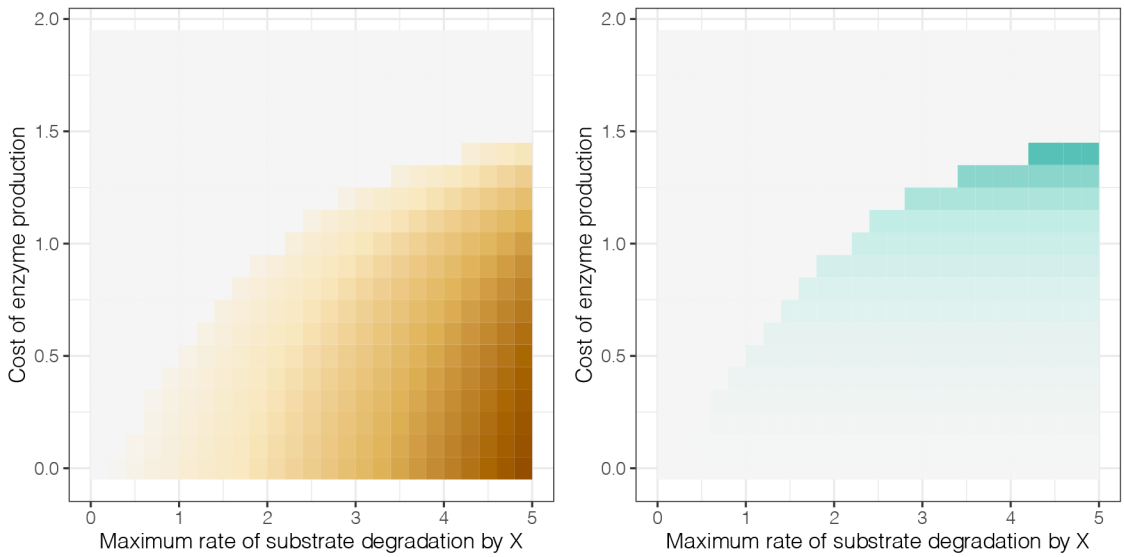

Figure 1: Densities at equilibrium of the producer species X (left) and of the cheater species A (right) as a function of the maximum rate of substrate degradation by X (c)and the cost of enzyme production on the growth rate of X (ϵ) for $k = 50$ (high flow of substrate between regional and local pools).

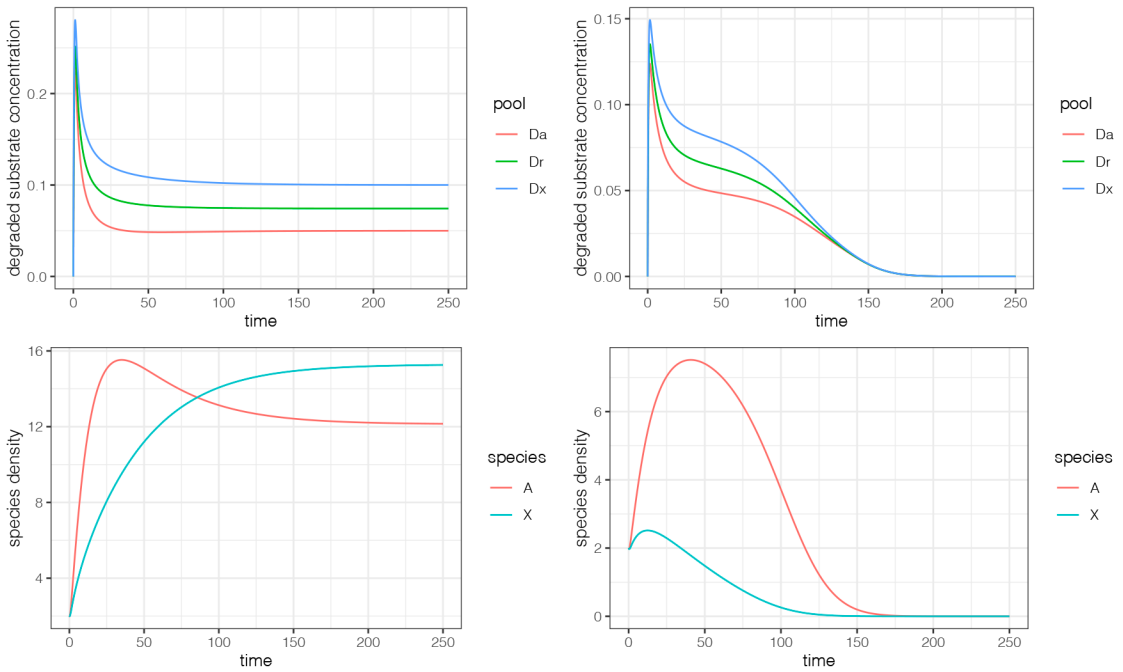

Figure 2: Temporal dynamics of the species densities and the concentration of degraded substrate in the local and regional pools in two case studies with $k = 50$ and $\epsilon = 1$. Left panels: Coexistence of X and A at equilibrium ($c = 3$). Right panels: Extinction of both X and A ($c = 1$).

907 **Table S1:** Strains description.

908

Species	Strain	Isolated from	year	Genome accession
P. aquaticum	A101-S19-F16	River water	2016	GCA_003382625.2
P. aquaticum	A127-S21-F16	River water	2016	GCA_003382655.2
P. aquaticum	A212-S19-A16^T	River water	2016	GCA_003382565.3
P. versatile	A73-S18-O15	River water	2015	GCA_020865565.1
P. versatile	CFBP5663	*Iris*	1983	GCA_004296765.1
P. versatile	CFBP6051^T	*solanum tuberosum*	NA	GCA_004296685.1
D. dianthicola	MIE34	Not available		GCA_009874285.1
D. dianthicola	CFBP2015	*Solanum tuberosum*	1975	GCA_009873535.1
D. dianthicola	CFBP1888	*Solanum tuberosum*	1978	GCA_009873515.1
D. solani	CC3239	Not available		Not available
D. solani	PPO9019	Not available		GCA_002846995.1
D. solani	CFBP8199^T	*solanum tuberosum*	2007	Not available
P. parmentieri	CFBP8475^T	*solanum tuberosum*	2008	GCA_001742145.1
P. parmentieri	CFBP5382	*solanum tuberosum*	1997	Not available
P. parmentieri	CFBP1338	*solanum tuberosum*	NA	Not available
P. atrosepticum	CFBP1453	*Lycopersicon esculentum*	1973	Not available
P. atrosepticum	CFBP1527	*solanum tuberosum*	1973	Not available
P. atrosepticum	CFBP7375	*solanum tuberosum*	2004	Not available
P. brasiliense	CFBP5381	*solanum tuberosum*	1997	GCA_013449475.1
P. brasiliense	CFBP3230	*Gossypium sp.*	1964	GCA_013449485.1
P. brasiliense	CFBP6617^T	*solanum tuberosum*	1999	GCA_009873295.1
P. carotovorum	CFBP1402	*Capsicum annuum*	1972	GCA_013449385.1
P. carotovorum	CFBP6074	*solanum tuberosum*	NA	GCA_013449495.1
P. carotovorum	CFBP2046^T	*solanum tuberosum*	1952	GCA_000749855.1 *
P. polaris	CFBP1403	*Helianthus annuus*	1969	Not available
P. parvum	CFBP8630^T	*solanum tuberosum*	NA	GCA_900195285.2
P. parvum	CFBP6058	*solanum tuberosum*	NA	GCA_000749915.1

909 * Deposited under the name NCPPB312

910

911 **Table S2:** Intra-species strain discrimination with the 341 nt gapA barcode.

912

species	strain	Nb of strain specific nucleotide (primer excluded)	Intra-species discrimination
P. aquaticum	A101	1	Discriminate the 3 strains
P. aquaticum	A127	1	
P. aquaticum	A212-ST	0	
P. versatile	A73E	0	Discriminate CFBP5663
P. versatile	CFBP5663	2	
P. versatile	CFBP6051^{T}	0	
D. dianthicola	MIE34	0	No discrimination
D. dianthicola	CFBP2015	0	
D. dianthicola	CFBP1888	0	
D. solani	CC3239	0	No discrimination
D. solani	PPO9019	0	
D. solani	CFBP8199^{T}	0	
P. parmentieri	CFBP8475^{T}	1	Discriminate CFBP8475
P. parmentieri	CFBP5382	0	
P. parmentieri	CFBP1338	0	
P. atrosepticum	CFBP1453	0	Discriminate CFBP7375
P. atrosepticum	CFBP1527	0	
P. atrosepticum	CFBP7375	22	
P. brasiliense	CFBP5381	0	Discriminate the 3 strains
P. brasiliense	CFBP3230	3	
P. brasiliense	CFBP6617^{T}	2	
P. carotovorum	CFBP1402	0	Discriminate CFBP2046
P. carotovorum	CFBP6074	0	
P. carotovorum	CFBP2046^{T}	2	
P. polaris	CFBP1403	0	No discrimination
P. parvum	CFBP8630^{T}	0	
P. parvum	CFBP6058	0	

913